ELEMENTA
Science of the Anthropocene

Darnis, G, et al. 2022. Zooplankton assemblages along the North American Arctic: Ecological connectivity shaped by ocean circulation and bathymetry from the Chukchi Sea to Labrador Sea. *Elem Sci Anth*, 10: 1. DOI: https://doi.org/10.1525/elementa.2022.00053

RESEARCH ARTICLE

Zooplankton assemblages along the North American Arctic: Ecological connectivity shaped by ocean circulation and bathymetry from the Chukchi Sea to Labrador Sea

Gérald Darnis[1,2,*], Maxime Geoffroy[2,3], Thibaud Dezutter[1], Cyril Aubry[1], Philippe Massicotte[4], Tanya Brown[5], Marcel Babin[4], David Cote[6], and Louis Fortier[1]

We defined mesozooplankton biogeography in the North American Arctic to elucidate drivers of biodiversity, community structure, and biomass of this key component of the Arctic marine ecosystem. A multivariate analysis identified four mesozooplankton assemblages: Arctic-oceanic, Arctic-shelf, Coastal-Hudson, and Labrador Sea. Bathymetry was a major driver of the distribution of these assemblages. In shallow waters, Cirripedia and the copepod *Pseudocalanus* spp. dominated the Coastal-Hudson and Arctic-shelf assemblages, which showed low species richness (19) and biomass (0.28 and 1.49 g C m^{-2}, respectively). The Arctic-oceanic assemblage occupied the entire North American Arctic, except for shallow breaks in the Canadian Arctic Archipelago downstream of sills blocking the Atlantic Water layer circulation below a depth of 200 m. This assemblage showed high copepod biomass (4.74 g C m^{-2}) with a high share of *Calanus hyperboreus*, *C. glacialis*, and *Metridia longa*. In habitats below 200-m depth, *C. hyperboreus* represented 68% of the copepod biomass, underscoring its role as a keystone species in this ecosystem. Strong numerical representation by the boreal-Atlantic *C. finmarchicus* and *Oithona atlantica* stressed the strong Atlantic influence on the subarctic Labrador Sea assemblage on the northwestern Labrador Sea slope. The mixed Arctic-Atlantic composition of the Labrador Sea mesozooplankton resulted in high species richness (58) and biomass (5.73 g C m^{-2}). The low abundance of Atlantic and Pacific taxa in the areas influenced by Arctic currents did not alter the Arctic status of the Arctic-oceanic, Arctic-shelf, and Coastal-Hudson assemblages. This study identifies hotspots of mesozooplankton biomass and diversity in Central Amundsen Gulf, Lancaster Sound, North Water Polynya and Baffin Bay, known for their high biological productivity and concentrations of vertebrate predators. The continental-scale zooplankton mapping furthers our understanding of the importance of bathymetry and ocean circulation for ecological connectivity in a vast and complex portion of the Arctic marine ecosystem.

Keywords: Mesozooplankton, Ecological connectivity, Biodiversity, North American Arctic, Arctic marine ecosystem

Introduction

Zooplankton constitutes a crucial component of the Arctic marine ecosystem, largely due to the different functional traits among a diversity of species. They contribute in various ways to ecosystem processes, including: 1) trophodynamics in the pelagic food web, but also in the benthic food web through the modulation of benthic-pelagic coupling (Darnis et al., 2012); 2) biogeochemical cycling of carbon, nitrogen, and other elements (Forest et al., 2011; Darnis et al., 2017); and 3) flow of pollutants in the system (Wang et al., 2018; Botterell et al., 2022). Arctic-endemic species like the large copepods *Calanus glacialis* and *C.*

[1] Pavillon Alexandre Vachon, Université Laval, Québec, QC, Canada
[2] Centre for Fisheries Ecosystems Research, Fisheries and Marine Institute of Memorial University of Newfoundland, St. John's, NL, Canada
[3] Faculty of Biosciences, Fisheries and Economics, UiT The Arctic University of Norway, Tromsø, Norway
[4] Takuvik International Research Laboratory, Université Laval (Canada) & Centre National de la Recherche Scientifique (France), Québec-Océan/Pavillon Alexandre-Vachon, Université Laval, Québec, QC, Canada
[5] Fisheries and Oceans Canada, Pacific Science Enterprise Centre, West Vancouver, BC, Canada
[6] Fisheries and Oceans Canada, Northwest Atlantic Fisheries Centre, St. John's, NL, Canada

* Corresponding author:
Email: gerald.darnis@qo.ulaval.ca

hyperboreus can exert strong grazing pressure on primary production in the top layer of the ocean (Tremblay et al., 2006) and build up large lipid reserves for reproduction and overwintering at depth (Falk-Petersen et al., 2009; Darnis et al., 2019). In turn, these energy-rich organisms with a pan-Arctic distribution constitute important prey for key fish species like Arctic cod (*Boreogadus saida*; Bouchard and Fortier, 2020), but also planktivorous birds (Pedersen and Falk, 2001; Karnovsky et al., 2011), and the bowhead whale (Carroll et al., 1987). Other numerically dominant small zooplankton taxa are essential prey for larval stages of carnivorous zooplankton and fish, and they also contribute greatly to organic matter remineralization in the water column (Darnis and Fortier, 2012; Halfter et al., 2020).

The geographic distribution of planktonic organisms across the pelagic realm is primarily regulated by large-scale ocean circulation (Oziel et al., 2020; Richter et al., 2020). Ocean currents are in turn generated by a complex interplay of physical processes involving the Coriolis effect, winds, waves, tides, differences in temperature, salinity, atmospheric pressure, and coastal and bottom topography. At high latitudes, sea ice affects underlying currents by modifying the momentum transfer from the atmosphere to the ocean and changing water properties through seasonal melting (Schulze and Pickart, 2012; Armitage et al., 2020). The vertical distribution and migrations of zooplankton through the water column also impact their transport across, or retention in, habitats where current shifts occur or where water layers set the conditions for current shears (Kimmerer et al., 2014). The complexities of seawater current patterns and dearth of oceanographic data make the study of the effect of transport mechanisms on zooplankton geographic distribution an extremely challenging endeavor in the Arctic. Nonetheless, studies at a regional scale have shown that environmental variables informing about water mass origin and vertical distribution, such as bathymetry, salinity, temperature, and water chemistry, could explain some of the variability in zooplankton community structure in the Chukchi and Beaufort seas and Hudson Bay (Rochet and Grainger, 1988; Darnis et al., 2008; Pomerleau et al., 2014; Smoot and Hopcroft, 2016).

A holistic description of zooplankton biogeography across large arctic marine ecosystems will contribute to understanding ecological connectivity in this region (Hillman et al., 2018) and facilitate predictions of ecosystem responses to stressors such as climate change. While local studies have described zooplankton community structure, abundance and biomass distribution in different habitats of the North American Arctic (Fortier et al., 2002; Ringuette et al., 2002; Ashjian et al., 2003; Hopcroft et al., 2005; Darnis et al., 2008), a lack of large-scale perspectives on zooplankton assemblages remains. This study provides a comprehensive assessment of mesozooplankton biogeographic patterns, in particular zooplankton community and biomass distribution, based on 409 sampling stations across the North American Arctic and eastern Subarctic, from the northern Chukchi Sea to coastal Labrador. We addressed the expectation that the Pacific and Atlantic influences on the western and eastern sides of the North American Arctic, respectively, create a longitudinal gradient in the zooplankton community structure. The potential influence of environmental factors on the distribution of zooplankton assemblages and key taxa were assessed to identify the main drivers of mesozooplankton community structure.

Methods

Study area

The maritime region under study is approximately 2,500,000 km^2 and spans a distance of 12,000 km from the westernmost station north of the Bering Strait to the southeasternmost one on the Labrador coast (**Figure 1**). From west to east, recognisable areas include: 1) the northern Chukchi Sea; 2) the shelf to basin areas of the Beaufort Sea, extending to the deep southern part of the Canada Basin; 3) the intricate network of channels of the Canadian Arctic Archipelago (CAA); 4) the North Water Polynya at the northern tip of Baffin Bay; 5) Baffin Bay, excluding the west Greenland shelf; 6) the Hudson Complex, grouping Foxe Basin, Hudson Strait and Hudson Bay; 7) the northwestern slope of the Labrador Sea, along a longitudinal transect centered on 60.46°N; and 8) four Labrador northern fjords (**Figure 1**; Table S1). Several sills of varying depths (18–675 m) cut the study region across narrow straits, starting with the Bering Sea to the west and ending with the much deeper Davis Strait to the southeast (**Figure 1a**).

Generally, the water column of the North American Arctic is stratified and composed of three main layers: the Polar Mixed Layer (0–50 m deep) of variable salinity and locally influenced by freshwater from rivers and sea-ice melt, the Pacific Halocline (50–200 m), and the relatively warm (>0°C) and saline Atlantic Water (>200 m) in deeper areas (Carmack and Macdonald, 2002). Pacific Water flows northward through the shallow and narrow Bering Strait (approximately 50 m deep and 80 km wide; **Figure 1a**). Flow through the CAA is complex and far from being fully resolved (McLaughlin et al., 2004). Because of the difference in sea levels, the flow direction is a generally southeastward from the Chukchi Sea and deep Canada Basin of the Arctic Ocean through the CAA, connecting the Beaufort Sea Gyre with its large freshwater reservoir and the western Labrador Sea (Rudels, 2015; Zhang et al., 2021). Due to the shallow topographic obstacles along the way, the Atlantic Water from the Arctic Ocean cannot flow through the CAA (Niemi et al., 2019). However, upper-slope water intrusions have been observed over the Canadian Beaufort Sea, Lancaster Sound and the North Water (see figure 1A of Bluhm et al., 2020). At the eastern border in Baffin Bay, the West Greenland Current flows from the Atlantic toward northern Baffin Bay along the west coast of Greenland (Münchow et al., 2015). Arctic water enters Hudson Bay through the shallow and narrow Fury and Hecla Strait in northern Foxe Basin and through northern Hudson Strait, while the outflow of water from the Hudson Complex is mainly through southern Hudson Strait (Loewen et al., 2020). The annual mean circulation in Hudson Bay remains cyclonic, because of the strong currents in autumn and winter and despite the weak anticyclonic flow in summer (Ridenour et al., 2019). Discharge

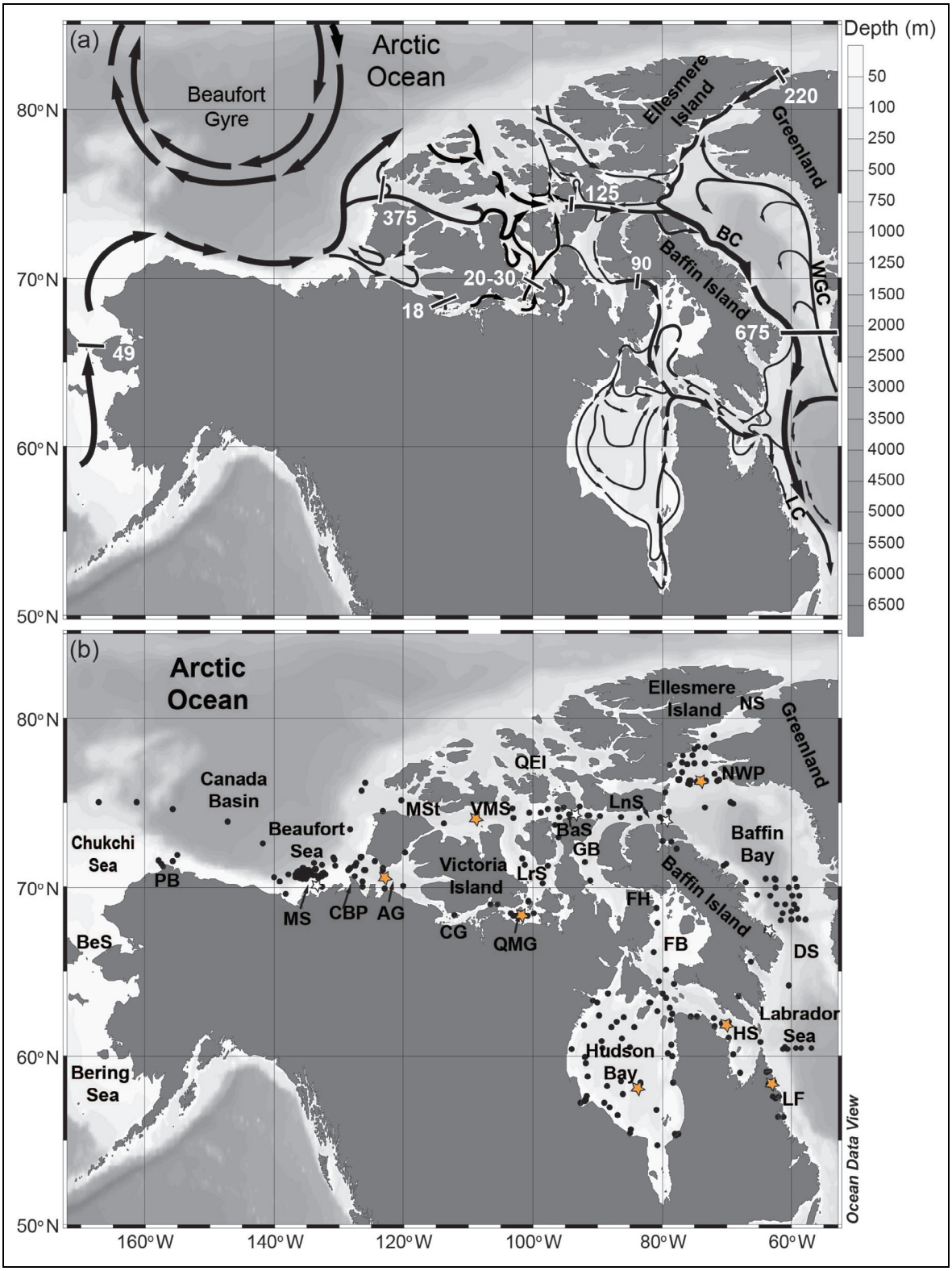

Figure 1. Near-surface circulation, sill locations, and zooplankton stations in the North American Arctic. (a) Schematic of water circulation adapted from Cuny et al. (2002), McLaughlin et al. (2004), Niemi et al. (2019), and Ridenour et al. (2019). Numbers in white font next to short black lines indicate sill depth. (b) Location of zooplankton stations sampled from 2005 to 2018 during the ArcticNet annual campaigns. Orange stars indicate locations of stations for the time series of ice concentration illustrated in Figure S1. Regions abbreviated: Amundsen Gulf (AG), Baffin Current (BC), Barrow Strait (BaS), Bering Strait (BeS), Coronation Gulf (CG), Davis Strait (DS), Foxe Basin (FB), Fury and Hecla Strait (FH), Gulf of Boothia (GB), Cape Bathurst Polynya (CBP), Hudson Strait (HS), Labrador Current (LC), Labrador fjords (LF), Larsen Sound (LrS), Lancaster Sound (LnS), Mackenzie Shelf (MS), M'Clure Strait (MSt), North Water Polynya (NWP), Nares Strait (NS), Point Barrow (PB), Queen Elizabeth Islands (QEI), Queen Maud Gulf (QMG), Viscount Melville Sound (VMS), and West Greenland Current (WGC).

of large river systems strongly affects temperature, salinity, colored dissolved organic matter, ambient light, ice dynamics, and pelagic primary production in several shallow neritic sectors of the study region, including the Mackenzie Shelf, South Kitikmeot, and Hudson Bay (Carmack and Macdonald, 2002; Tremblay et al., 2019; Dezutter et al., 2021). On the southeastern limits of the study region, the northwestern Labrador Sea is considered a confluence area under the influences of both the cold southward-flowing Labrador Current and a section of a recirculation cell of the North Atlantic and West Greenland Current (Cuny et al., 2002).

Sea ice coverage in the North American Arctic is a mixture of seasonal and multiyear ice (Michel et al., 2015). Most of the multiyear ice originates from the central pack ice and flows from the Arctic Ocean through M'Clure Strait, the Queen Elizabeth Islands passages, and Nares Strait once the landfast ice in the CAA has melted during spring–autumn (Howell et al., 2013). The regime of seasonal ice cover is extremely variable, spatially and temporally, over this vast region and the duration and extent of sea ice has decreased considerably in the past decades (Mudryk et al., 2018). The northwestern portion of the Parry Channel, including M'Clure Strait and Viscount Melville Sound, has the thickest sea ice and longest ice duration of the study region, whereas the easternmost stations in the North Atlantic Labrador Sea are almost ice-free year-round, being at the limit of the North American seasonal ice perimeter (Environment and Climate Change in Canada, 2021).

The North American Arctic is considered oligotrophic, with short phytoplankton blooms constrained to the spring–summer period (Michel et al., 2015). However, some areas are recognized for their high biological production, such as the Cape Bathurst Polynya and central Amundsen Gulf in the southeastern Beaufort Sea, Lancaster Sound, and the North Water Polynya in northern Baffin Bay (Ardyna et al., 2011). The annual pelagic primary production in the subarctic Labrador Sea is similar to the estimates made in the areas mentioned above (Tremblay et al., 2006; Forest et al., 2011; Harrison et al., 2013). On the other hand, annual primary production is low in the Canada Basin, Hudson Bay, and South Kitikmeot which comprises the Queen Maud Gulf area at the centre of the CAA (Lee and Whitledge, 2005; Tremblay et al., 2019; Back et al., 2021). The annual cycle of photosynthetically based primary production is initiated by ice algae when sufficient photosynthetically active radiation (PAR) reaches the bottom of sea ice in early spring. An under-ice phytoplankton bloom may start after snow melt above first-year sea ice, followed by open-water blooms if nutrient concentrations remain high enough in the surface layer (Ardyna and Arrigo, 2020). As nutrients get consumed and depleted throughout the ice-free season, subsurface chlorophyll maxima form and follow a deepening nitracline (Martin et al., 2010).

Remote sensing

Daily-average sea ice concentrations were retrieved at a spatial resolution of 12.5 km from the Centre ERS d'Archivage et de Traitement (CERSAT) of the French Research Institute for the Exploitation of the Sea (e.g., see methods in Dezutter et al., 2021). Annual surface chlorophyll-a (Chl-a) concentrations were extracted from MODIS-Aqua at a spatial resolution of 4 km (https://oceancolor.gsfc.nasa.gov/). Chl-a derived from the Garver–Siegel Maritorena (GSM) algorithm was preferred over the band-ratio algorithm because it performs better in coastal areas influenced by terrestrial inputs (Clay et al., 2019).

Sampling

This work builds on a large dataset collected from 2005 to 2018 as part of the ArcticNet collective multiannual field programs across the Canadian Arctic (Table S1). In 2014, transit through the Bering Strait from the Pacific allowed sampling in the northern Chukchi Sea, western Beaufort Sea, and deep Canada Basin, Western Arctic. The annual sampling period changed from year to year. The earliest and latest sampling days were June 1 (in 2018 in Hudson Strait) and November 13 (in 2009 in Anaktalak fjord in Labrador), respectively. The biogeographic study is based on 409 zooplankton samples collected at 283 geographic sites. Forty-four of these sites spread throughout the Canadian Arctic were sampled several times over the 14 years of the study.

Zooplankton sampling procedures are described in Darnis et al. (2008) and Darnis and Fortier (2012). Most of the zooplankton samples were collected using a 4-net sampler consisting of four 1-m^2 aperture, 4.5-m long, conical-square plankton nets (two nets of 200-μm mesh and two of 500-μm mesh size) mounted side by side on a 2x2-m metal frame. For <9% of the deployments, a 0.5-m^2 square aperture Hydrobios Maxi® multinet sampler was used instead of the 4-net sampler. The multinet carried nine 4.5-m long nets of 200-μm mesh size. Nets of both gears were fitted with 2-L rigid codends and the samplers were deployed in the same way. The multinet casts were done at various sites covering a large part of the study region, from the Beaufort Sea to the west, to Baffin Bay and the Labrador Sea to the southeast. Immediately after the CTD cast, the sampler was lowered codend first to avoid filtration on the downward trajectory. After a 1-min pause at 10 m above the sea floor, the sampler was hauled vertically to the surface at a speed of 0.5 m s^{-1}. The nine nets of the multinet were deployed sequentially to assess zooplankton vertical distribution, described by Darnis and Fortier (2014). Due to many technical malfunctions of the different flowmeters mounted on the two sampling gears, we assumed 100% filtration efficiency by the nets. Upon retrieval, macrozooplankton (large amphipods, euphausiids, medusae and fish larvae) were removed, as they are not sampled quantitatively by the vertical tows. For this study, only the samples from the 200-μm mesh nets of the 4-net sampler and multinet were preserved in a borax-buffered seawater solution of 4% formaldehyde for taxonomic identification. A Sea-Bird SBE 911plus CTD system with an auxiliary SeaPoint chlorophyll fluorometer, integrated with a carousel water sampler, provided water-column profiles of salinity, temperature, and fluorescence.

Laboratory analysis

The formalin-preserved samples were rinsed, size-fractionated on a 1000-µm sieve, and resuspended in distilled water. Successive aliquots were taken from the 200–1000-µm size fraction using a Henson-Stempel pipette, and the 1000-µm fraction using a Motoda splitting box, until 300 animals from each fraction were counted and identified to species or to the lowest possible taxonomic level under the stereomicroscope. Only the prosome length of copepods was measured and recorded for morphometric purposes. The congeneric species *Calanus glacialis* from the Arctic and the subarctic-Pacific *C. marshallae* were pooled in a single *C. glacialis* taxon because of uncertainties in differentiating them. For similar reasons, members of the genus *Microcalanus* and *Pseudocalanus* were not identified to species. Carbon content for each copepod taxon was calculated using published prosome length-mass relationships for arctic zooplankton (Mumm, 1991; Hopcroft et al., 2005; Forest et al., 2010). Each sample from the water-column stratifying multinet sampler was processed as described above, and the zooplankton counts from the different layers at a station were pooled to estimate a water-column integrated abundance of individuals (ind) per meter squared.

Data analysis

Patterns in zooplankton community structure were explored through multivariate analyses using a species by station matrix of water-column integrated abundance from the 200-µm plankton net vertical tows pooled across all years. The multivariate analyses were conducted using the PRIMER V6® software package (PRIMER-E Ltd, Plymouth, UK). The integrated abundance was expressed as a proportion (the ratio of taxon abundance to total abundance) to attenuate the effects of large variation in filtered volumes due to the extensive depth range (26–3860 m; Darnis et al., 2008). The proportion matrix was square-root arcsine-transformed to balance the weights between highly abundant taxa and taxa likely to have been undersampled (appendicularians, cnidarians and ctenophores). Station similarity in zooplankton composition was assessed using the Bray-Curtis similarity index (Bray and Curtis, 1957). A cluster analysis using the group average mode was applied to the resemblance matrix to identify groupings of stations based on similarity in zooplankton composition. Significant faunal clusters were identified using the SIMPROF routine (significance at $\alpha = 0.05$). A non-metric multidimensional scaling (NMDS) ordination was applied to the same similarity matrix to produce a visual representation of the faunal similarities of the stations in two dimensions. The NMDS ordination is associated with a stress coefficient that measures the divergence between the data and its representation. A stress value <0.2 generally indicates a good representation of the proximity of taxonomic composition for all pairs of samples (Clarke and Warwick, 2001). The similarity of percentage (SIMPER) routine was carried out to identify the taxa most responsible for the intra-assemblage similarity and dissimilarity among zooplankton assemblages revealed by the cluster and NMDS analyses.

Two approaches were taken to identify the environmental conditions that influenced the geographic distribution of the zooplankton assemblages. First, multiple linear regressions were made to relate environmental data to the coordinates of the stations on the ordination produced by the NMDS, following Kruskal and Wish (1978). Each environmental variable was used as the dependent variable and the coordinates for the two axes of the NMDS plot, summarizing the ecological data, as the independent variables. The environmental variables considered included station depth, water-column mean salinity, temperature, and mean fluorescence, surface (0–10 m) salinity and temperature, mean annual surface Chl-a concentration, depth of fluorescence maximum, day of sampling, year of sampling, latitude, longitude, summer ice-free season, ice-free period from ice breakup to zooplankton sampling, ice breakup day (i.e., first day of year when ice was <50%). The times when sea ice reached 50% concentration were used to indicate ice breakup and freeze-up in our study region (Darnis et al., 2008). For the second analytical approach, the BEST/BIO-ENV function of the PRIMER software and Spearman's rank correlation coefficient were used to explore correlations between the above environmental variables and the biotic similarity matrix.

Results

Environmental conditions

The annual time series of ice concentration from 2005 to 2018 at selected sites across the section studied illustrates the large spatial, seasonal, and interannual variability in ice coverage over the study region (**Table 1**; Figure S1). The Stations 186, 145, and 199 (Table S1) showed the shortest ice-free seasons averaged over the years 2005–2018 (<100 days) in Viscount Melville Sound on the northwestern branch of the Northwest Passage, the South Kitikmeot on the southwest branch of the Northwest Passage, and Barrow Strait at the centre of the CAA, respectively. Station 186 also had the latest sea-ice breakup and earliest freeze-up (**Table 1**). At the western border of the CAA, Station 66 on the Mackenzie Shelf and Station 111 in Amundsen Gulf showed sea-ice regimes similar to Station 215 in Lancaster Sound at the eastern border of the CAA, with ice breakup in late May–early June and freeze-up in late October–early November. On a north–south gradient in the eastern part of the study region, the open-water season in the high Arctic North Water (Station 256) lasted longer than at the Lancaster Sound station and at Station 305 along the coast of Baffin Island, located almost 10 degrees of latitude south of the polynya station. The northernmost station had the earliest sea-ice breakup (mid-May) of the 11 selected stations across the study region. However, the subarctic stations in Hudson Strait and in Saglek Fjord of the Labrador Sea had the latest freeze-up and the longest open-water season.

Bathymetry varied from 26 m (Foxe Basin in 2017) to 3860 m (Canada Basin in 2014) along the track of the ship, which differed across years (**Figures 2**, **3**, and S2). Throughout the sampling areas and years, the thin Polar Mixed Layer at the top of the water column was

Table 1. Average dates ± standard deviation of sea-ice breakup, freeze-up, and duration of the ice-free season in the North American Arctic and eastern Subarctic over the annual cycles of 2005–2018

Region	Station[a]	Ice Breakup Date (Julian Day)	Ice Freeze-Up Date (Julian Day)	Ice-Free Season (Days)
Mackenzie Shelf	66	156 ± 23	300 ± 08	144 ± 25
Amundsen Gulf	111	154 ± 25	308 ± 06	154 ± 23
South Kitikmeot	145	203 ± 06	299 ± 07	96 ± 12
Viscount Melville Sound	186	233 ± 14	262 ± 10	29 ± 19
Barrow Strait	199	186 ± 37	282 ± 11	96 ± 40
Lancaster Sound	215	147 ± 13	292 ± 07	145 ± 17
North Water Polynya	256	132 ± 10	300 ± 09	168 ± 15
West Baffin Bay	305	200 ± 11	320 ± 07	119 ± 14
Hudson Strait	316	159 ± 12	348 ± 14	189 ± 22
Central Hudson Bay	359	183 ± 08	339 ± 06	156 ± 07
Coastal Labrador	387	157 ± 20	372 ± 14	215 ± 24

[a]Station locations and sampling dates provided in Table S1.

characterized by variable temperature (**Figure 2**) and salinity levels (**Figure 3**), varying with the location and date of sampling. This variability was particularly evident for surface salinity, which tended to be low (25–30) in areas influenced by sea-ice meltwater and/or river plumes, such as the Mackenzie Shelf, deep Canada Basin, South Kitikmeot, and Hudson Bay. Below the Polar Mixed Layer, the Pacific-origin Halocline had much more constant temperatures and salinities until about 200-m depth and could be observed from the west of the study region to the southeast, except in the Labrador Sea. With temperatures ranging from 0 to −1.7°C and salinities of 32–33, the Pacific Halocline was usually colder and more saline than the Polar Mixed Layer at the time of sampling and was situated above the Atlantic-origin Water mass where they overlapped. This Atlantic Water was characterised by above-zero temperatures and salinities >34, both higher than in the Polar Mixed Layer and Pacific Halocline. The Atlantic Water extended to depths of 1000 m where bathymetry allowed.

The surface Chl-a concentration, averaged over the ice-free period of each year, was low (1.14 ± 3.07 mg m^{-3}) and remained below 5 mg m^{-3} across most of the North American Arctic (**Figure 4**). Values above this threshold were found only in a few delimited shallow coastal areas, including Point Barrow to the west, the inner Mackenzie Shelf, eastern Queen Maud Gulf, and southern Hudson Bay.

Zooplankton abundance and biomass

The distribution of total zooplankton abundance showed high within-region variability but no obvious large-scale geographic patterns (**Figure 5**). The lowest integrated abundances (<10,000 ind m^{-2}) were observed over the Beaufort shelf and slope, and in Hudson Bay, whereas the highest abundances (>400,000 ind m^{-2}) were recorded in the Chukchi Sea, Amundsen Gulf, Queen Maud Gulf in the South Kitikmeot, Hudson Bay, and Labrador fjords. From the 201 mesozooplankton taxa identified in the 409 samples analyzed, only 14 taxa had an individual share of the zooplankton composition that was >1% of total abundance, averaged over the entire dataset (Table S2). The small copepod *Oithona similis* was the most abundant species and accounted for 29% of the entire zooplankton composition.

The oceanic taxa *Microcalanus* spp., *Triconia borealis*, *Metridia longa*, and *Calanus hyperboreus* combined had a share of 39 ± 15% (mean ± 1 standard deviation, SD) of the composition in the regions >200 m in depth, including the Canada Basin/Beaufort Sea, western and eastern borders of the Canadian Arctic Archipelago, Baffin Bay, and the centre of Hudson Strait (**Figure 5**; **Table 2**). Conversely, this group of species comprised only 15 ± 15% of the composition over the Chukchi Sea, South-Kitikmeot, Barrow Strait, Hudson Bay and Labrador fjords, all areas shallower than 200 m. By contrast with the oceanic taxa, the neritic *Pseudocalanus* spp. was more prevalent in the assemblage over the regions <200 m in depth, where this species complex made up 33 ± 19% of the assemblage by numbers, compared to 12 ± 10% at the 209 stations in the depth range of 200–3860 m. At the offshore stations in the Labrador Sea, *Pseudocalanus* spp. comprised only 1.3 ± 1.6% of the numerical composition, a small contribution compared to the 14 ± 8 and 10 ± 4% by the North Atlantic *Calanus finmarchicus* and *Oithona atlantica*, respectively, in this southernmost part of the study region on the Atlantic side. The large North Pacific copepods *Eucalanus bungii*, *Metridia pacifica*, and *Neocalanus* spp., were found in less than 1% of the stations sampled (**Table 2**). Only one specimen of *Neocalanus*

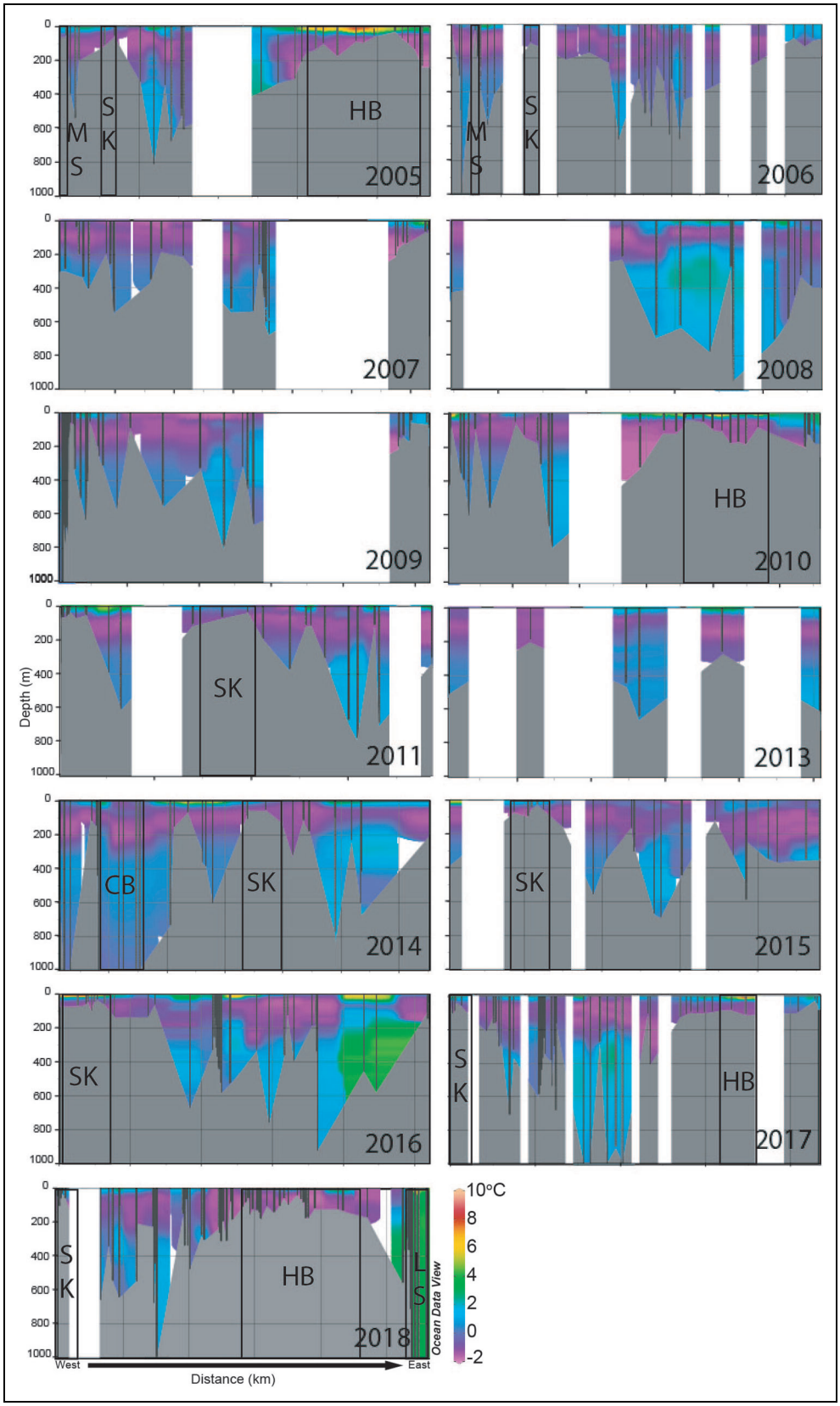

Figure 2. Time-depth sections of temperature in the North American Arctic from 2005 to 2018. All annual sections from the northwesternmost station to the southeasternmost station (see Figure S2). Annual variations of track distances are not shown on the x-axis. The Mackenzie Shelf (MS), South Kitikmeot (SK), Hudson Bay (HB), and Canada Basin (CB) are labelled to illustrate the strong influence of river runoff and meltwater on surface hydrography, and the Labrador Sea (LS) for the larger influence of the Atlantic Water layer south of Davis Strait.

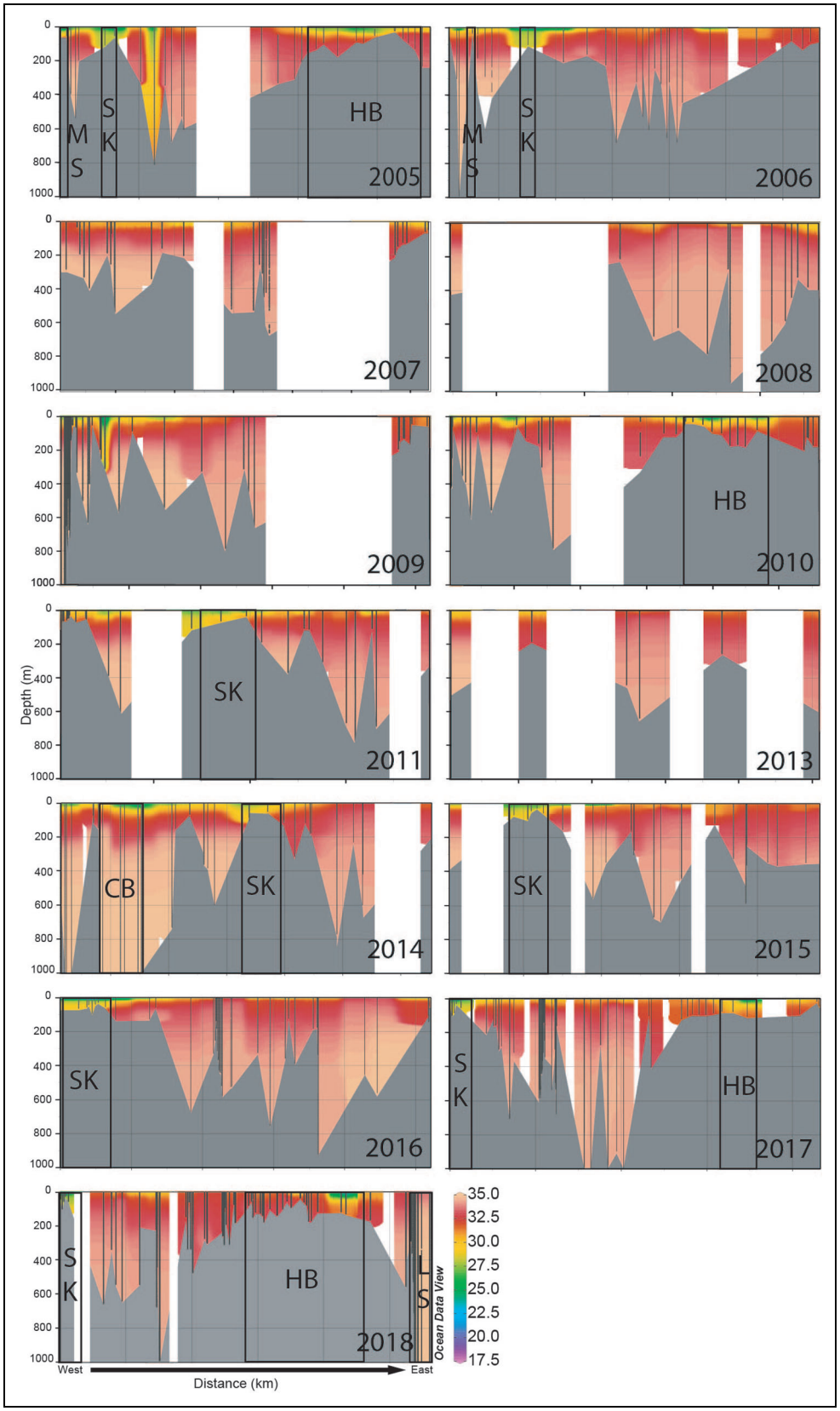

Figure 3. Time-depth sections of salinity in the North American Arctic from 2005 to 2018. All annual sections from the northwesternmost station to the southeasternmost station (see Figure S2). Annual variations of track distances are not shown on the x-axis. The Mackenzie Shelf (MS), South Kitikmeot (SK), Hudson Bay (HB), and Canada Basin (CB) are labelled to illustrate the strong influence of river runoff and meltwater on surface hydrography, and the Labrador Sea (LS) for the larger influence of the Atlantic Water layer south of Davis Strait.

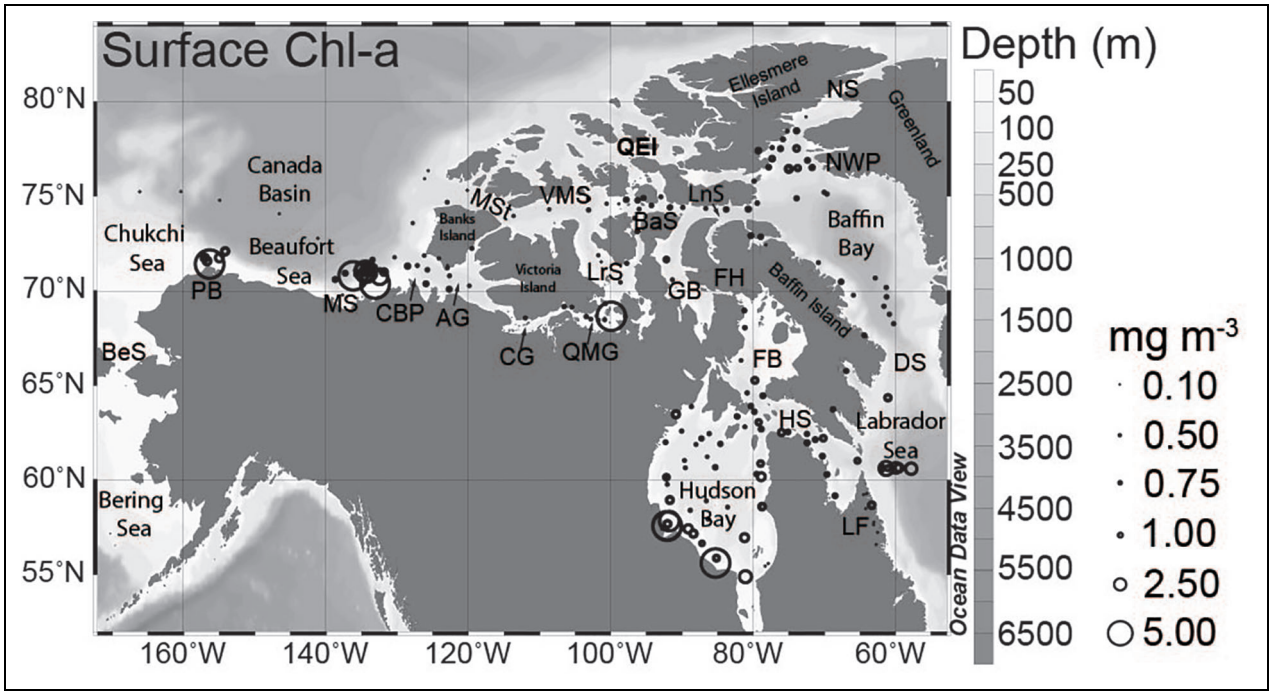

Figure 4. Distribution of annual mean surface Chl-a concentration across the North American Arctic. Circle size indicates Chl-a concentration, from 0.10 to >5.00 mg m^{-3}. Regions by abbreviation: Amundsen Gulf (AG), Barrow Strait (BaS), Bering Strait (BeS), Cape Bathurst Polynya (CBP), Coronation Gulf (CG), Davis Strait (DS), Foxe Basin (FB), Fury and Hecla Strait (FH), Gulf of Boothia (GB), Hudson Strait (HS), Labrador fjords (LF), Lancaster Sound (LnS), Larsen Sound (LrS), Mackenzie Shelf (MS), M'Clure Strait (MSt), North Water Polynya (NWP), Nares Strait (NS), Point Barrow (PB), Queen Elizabeth Islands (QEI), and Viscount Melville Sound (VMS).

spp. was identified at a station in the Chukchi Sea, while each of the other two species was found in low numbers at three stations in the Chukchi/western Beaufort Sea region in 2014. Euryhaline taxa indicative of brackish estuarine waters, such as *Acartia* spp., *Centropages* spp., *Eurytemora* spp. and *Limnocalanus* spp., were generally found at specific sites in the Chukchi and Beaufort Sea, South Kitikmeot, Barrow Strait, Hudson Bay, and the Labrador fjords. The occurrence of the three latter taxa was always sporadic, whereas *Acartia* spp. figured among the co-dominant taxa in Hudson Bay and in the Labrador fjords. Cirripedia meroplankton contributed >10% of zooplankton abundance at 23 stations <200 m in depth, among which 19 were in Hudson Bay (**Figure 5**; **Table 2**).

The spatial distribution of copepod biomass (**Figure 7**) showed obvious geographic disparities not observed for the distribution of zooplankton abundance (**Figure 5**). The mean biomass over the areas shallower than 200 m (including Chukchi and Beaufort shelves, South Kitikmeot region, Barrow Strait, Hudson Bay, and the Labrador Okak and Anaktalak fjords) was more than 4 times lower than in the deeper areas (Mackenzie continental slope, Amundsen Gulf, Lancaster Sound, North Water, Baffin Bay, Hudson Strait, and Labrador Sea), with 1.3 ± 1.7 versus 6.2 ± 3.9 g C m^{-2}, respectively. In regions repeatedly surveyed during the multi-year study period, the South Kitikmeot (3 sampling years, 46 stations and mean depth of 78 ± 31 m) and Hudson Bay (3 sampling years, 51 stations and mean depth of 111 ± 56 m) hosted copepod biomasses of 0.7 ± 0.5 and 0.5 ± 0.5 g C m^{-2}, respectively. These values were 8 to 10 times lower than estimates for the ArcticNet long-term observatories in the Amundsen Gulf (8 sampling years, 31 stations and mean depth of 425 ± 132 m) and the North Water (9 sampling years, 32 stations and mean depth of 480 ± 128 m) that hosted biomasses of 6.2 ± 3.6 and 7.9 ± 3.9 g C m^{-2}, respectively.

Furthermore, the large copepods *Calanus hyperboreus, C. glacialis*, and *Metridia longa* generally exceeded 80% of the biomass but <15% of the abundance, while the much smaller copepods *Oithona similis*, *Pseudocalanus* spp., *Microcalanus* spp., and *Triconia borealis* contributed >65% of the numerical composition but only 12% of the biomass in the entire study region (**Figures 5** and **7**). *C. glacialis*, *C. hyperboreus*, *Pseudocalanus* spp., and *M. longa* accounted for 35, 31, 17, and 7%, respectively, of the copepod biomass in the areas shallower than <200 m. On the other hand, *C. hyperboreus* alone made up 68% of the biomass where depths were >200 m, followed by *C. glacialis* and *M. longa* (15 and 11%, respectively). *Pseudocalanus* spp. had a low contribution of <1% in the deep zones of the study region. In Amundsen Gulf and the North Water, on either side of the CAA, biomass compositions were similar and illustrative of biomass of the deep areas described above. However, compositions clearly differed between the shallow areas of the South Kitikmeot at the centre of the CAA and Hudson Bay on the southeast subarctic side of the study area. In Hudson Bay, the contribution of *Calanus* spp. to biomass was

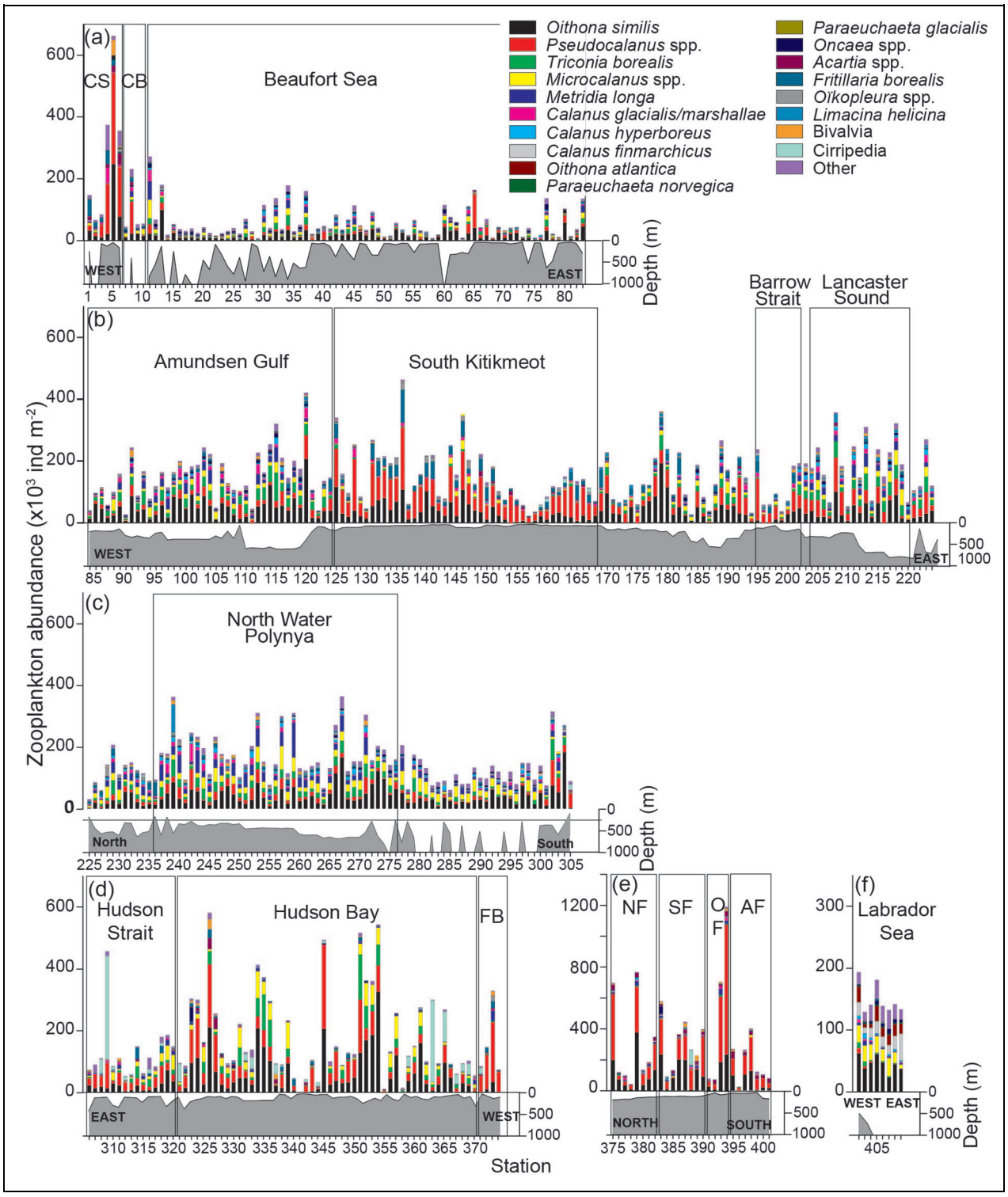

Figure 5. Contribution of main taxa to water-column integrated zooplankton abundance in the North American Arctic. The 409 stations sampled in the Western Arctic, including: (a) the Chukchi Sea (CS), Canada Basin (CB), and Beaufort Sea; (b) the Canadian Arctic Archipelago from Amundsen Gulf and South Kitikmeot to Barrow Strait and Lancaster Sound; (c) Baffin Bay from north to south; (d) the Hudson complex comprising Hudson Strait, Hudson Bay, and Foxe Basin (FB); (e) Labrador fjords, including Nachvak (NF), Saglek (SF), Okak (OF), and Anaktalak fjords (AF); and (f) the Labrador Sea, superimposed on the bathymetry of the respective regions of the American Arctic and Subarctic. Note the different scales of the abundance axis for the Labrador fjords and Sea.

half the contribution in the South-Kitikmeot, whereas biomass of *Pseudocalanus* spp. was double. Furthermore, the individual shares of the small copepods *Triconia borealis*, *Microcalanus* spp., and *Oithona similis* were 17, 10 and 3 times higher, respectively, in Hudson Bay than in the centre of the CAA.

Table 2. Taxa characteristic of the four main zooplankton assemblages[a] of the North American Arctic and eastern Subarctic, with total abundance, copepod biomass and diversity indices

		Abundance (x10^3 ind m^{-2})				Contribution (%)			
Taxon	**Occurrence (%)[b]**	**LS**	**CH**	**AOc**	**AS**	**LS**	**CH**	**AOc**	**AS**
Oithona similis	99	45.3	10.4	41.1	53.9	30	8	31	27
Pseudocalanus spp.	100	2.1	16.1	18.4	94.3	1	13	14	47
Triconia borealis	92	3.2	7.2	16.5	3.3	2	6	12	2
Microcalanus spp.	91	22.4	4.6	16.5	3.5	15	4	12	2
Metridia longa	93	3.0	0.7	11.5	2.5	2	1	9	1
Fritillaria borealis	62	0.6	0.8	2.6	14.4	<1	<1	2	7
Calanus glacialis	100	2.3	1.2	6.0	5.0	2	1	4	2
Cirripedia	47	<0.1	68.9	1.0	2.7	<1	56	1	1
Calanus hyperboreus	93	3.6	<0.1	4.1	1.0	2	<1	3	1
Acartia spp.	37	0	2.1	0.4	6.3	0	2	<1	3
Limacina helicina	81	<0.1	0.3	2.0	1.6	<1	<1	2	1
Oncaea notopus	50	0.4	0.1	2.2	1.0	<1	<1	2	<1
Oikopleura vanhoeffeni	75	0.6	0.3	1.4	2.8	<1	<1	1	1
Bivalvia	48	<0.1	1.6	1.5	2.5	<1	1	1	1
Polychaeta	75	1.1	1.5	0.8	1.8	1	1	<1	1
Calanus finmarchicus	43	20.4	<0.1	0.4	0.2	14	<1	<1	<1
Boroecia maxima	46	3.3	0	0.5	<0.1	2	0	<1	<1
Parasagitta elegans	73	<0.1	0.2	0.2	0.8	<1	<1	<1	<1
Oithona atlantica	6	15.9	0	<0.1	<0.1	11	0	<1	<1
Scolecithricella minor	35	2.6	0	0.4	<0.1	2	0	<1	0
Euphausiacea	16	0.4	5.2	<0.1	0.3	<1	4	<1	<1
Oncaea spp.	12	4.2	0	0.26	<0.1	3	0	<1	0
Spinocalanus sp.	5	3.9	0	0.1	<0.1	3	0	<1	<1
Chaetognatha	13	1.7	0.2	<0.1	<0.1	1	<1	<1	0
Paraeuchaeta norvegica	6	1.6	0	<0.1	0	1	0	0	0
Metridia lucens	1	<0.1	0	0	0	<1	0	0	0
Metridia pacifica	1	0	0	0	<0.1	0	0	0	0
Eucalanus bungii	1	0	0	0	<0.1	0	0	0	0
Neocalanus cristatus	<1	0	0	<0.1	0	0	0	0	0
Summing parameters									
Total abundance (x10^3 ind m^{-2})	–[c]	149	122	133	202	–	–	–	–
Copepod biomass (g C m^{-2})	–	5.73	0.28	4.74	1.49	–	–	–	–
Diversity indices									
Species richness (*S*)	–	58	19	26	19	–	–	–	–
Shannon-Wiener index (*H'*)	–	3.39	2.25	2.69	2.23	–	–	–	–

[a]Defined by cluster analysis (**Figure 6**) and designated Labrador Sea (LS), Coastal-Hudson (CH), Arctic-oceanic (AOc), and Arctic-shelf (AS) zooplankton assemblages.

[b]Percent occurrence of each taxon at the 409 sampling stations analyzed.

[c]Not applicable or available.

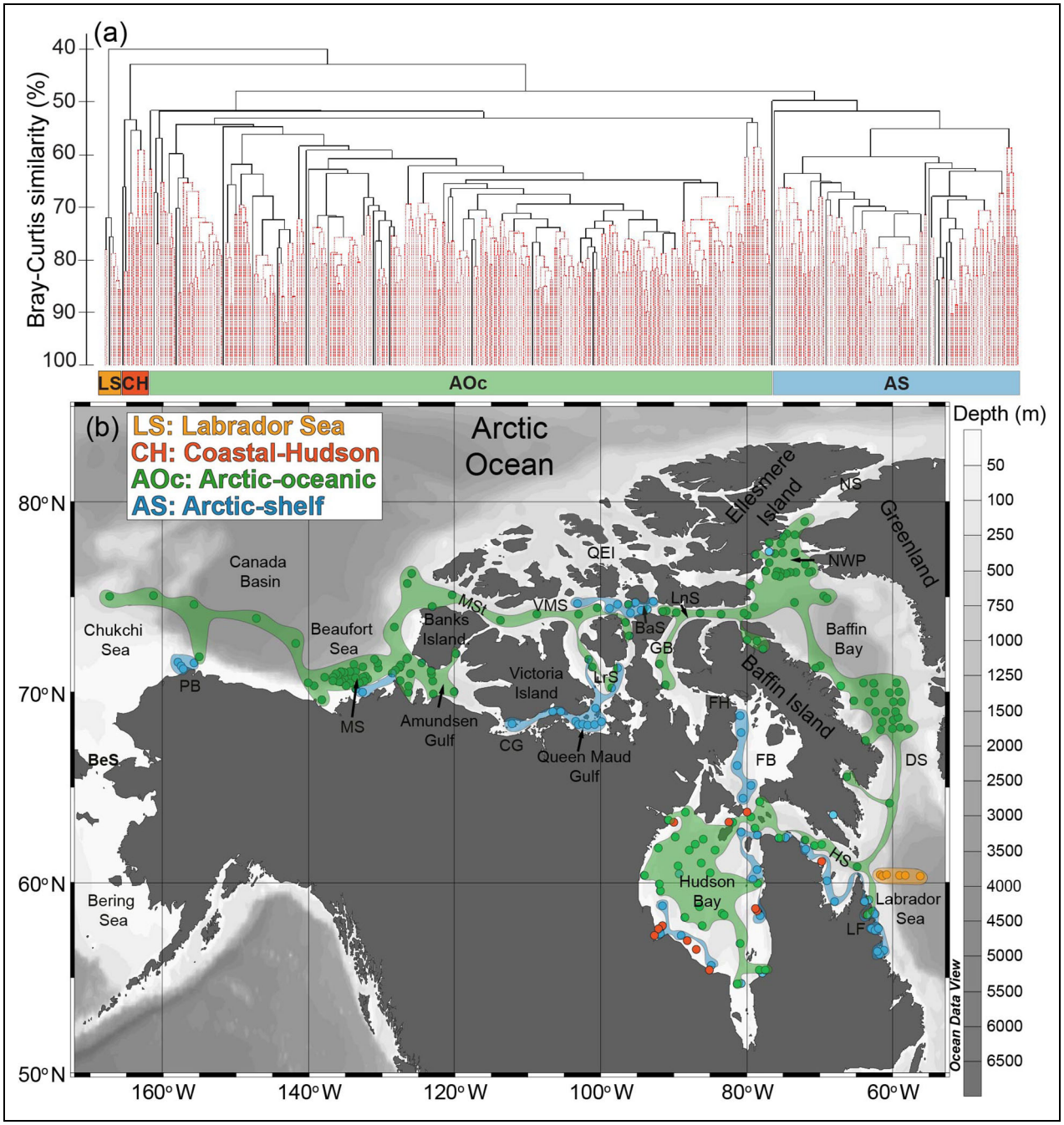

Figure 6. Main mesozooplankton assemblages in the North American Arctic and eastern Canadian Subarctic. (a) Clustering of the 409 stations sampled in the North American Arctic and subarctic Hudson Bay and Labrador Sea based on the relative abundance of mesozooplankton taxa. Black unbroken and red dotted lines of this dendrogram define, respectively, statistically significant and insignificant groupings of stations based on the SIMPROF significance test in PRIMER V6. (b) Geographical distribution of the mesozooplankton assemblages identified by the clustering analysis of the sampling stations in (a). Colored envelopes join stations of main assemblages for the Labrador Sea (LS), Coastal-Hudson (CH), Arctic-oceanic (AOc), and Arctic-shelf (AS). Regions abbreviated: Barrow Strait (BaS), Bering Strait (BeS), Coronation Gulf (CG), Davis Strait (DS), Fury and Hecla Strait (FH), Gulf of Boothia (GB), Hudson Strait (HS), Labrador fjords (LF), Lancaster Sound (LnS), Larsen Sound (LrS), Mackenzie Shelf (MS), M'Clure Strait (MSt), North Water Polynya (NWP), Nares Strait (NS), Point Barrow (PB), Queen Elizabeth Islands (QEI), and Viscount Melville Sound (VMS).

Hotspots of depth-integrated biomass were found mainly over the Mackenzie slope, central Amundsen Gulf, Lancaster Sound, the North Water, Baffin Bay, and the Labrador Sea and fjords (**Figure 8**). On the other hand, areas of relatively low biomass were detected in the northern Chukchi Sea/Canada Basin region, South Kitikmeot, Foxe Basin, and Hudson Bay. The distribution of *Calanus hyperboreus*, *C. glacialis*, *Metridia longa*, and *Paraeuchaeta*

spp. followed the total copepod biomass distribution described above (first panel of **Figure 8**). Biomass distribution of the boreal Atlantic *C. finmarchicus* was restricted to the eastern part of the study area, with highest biomasses observed in the Labrador Sea. The patterns of biomass distribution of *Pseudocalanus* spp. and the other small copepods differed from the ones displayed by the main large copepods. Hotspots of *Pseudocalanus* spp. biomass were more coastal, being in relatively shallow areas over the Chukchi Sea, South Kitikmeot, Hudson Bay, and the Labrador fjords. The two latter regions stand out as areas of higher biomass of small copepods.

Zooplankton community structure

The cluster analysis of the 409 stations based on zooplankton numerical composition revealed four distinct groups at the 50% similarity level (SIMPROF test; **Figure 6a**). The first group consisted of 8 stations along a longitudinal transect over the western slope of the Labrador Sea at about 60.5°N (**Figure 6b**) and was identified as the "Labrador Sea" (LS) assemblage. In this group, the dominant copepods *Oithona similis*, *Microcalanus* spp., *Calanus finmarchicus* and *O. atlantica*, represented 30, 15, 14 and 11%, respectively, of the total abundance of 149 ± 72 x10^3 ind m^{-2} (mean ± 1 SD; **Table 2**). The latter two taxa from the North Atlantic never comprised more than 0.3% of the other groups. Furthermore, they were ranked among the most important contributors to the differentiation of the LS assemblage from the others (SIMPER analysis; **Table 3**). Mesopelagic species such as the copepods *Spinocalanus* spp., *Scolecithricella minor*, *Paraeuchaeta norvegica*, *Gaetanus tenuispinus*, *Scaphocalanus brevicornis*, *Heterorhabdus norvegicus*, the amphipod *Themisto abyssorum*, and the ostracods *Boroecia maxima*, *Discoconchoecia elegans*, and *Obtusoecia obtusata* also contributed largely to the relatively high species richness of the LS group (58 taxa; **Table 2**). The neritic taxa *Pseudocalanus* spp., *Calanus glacialis*, *Acartia* spp. and the meroplankton Cirripedia, Bivalvia, and Echinodermata showed a lower share of the composition, compared to the other groups.

Eleven of the 12 stations in the second group were distributed around Hudson Bay, and the latter on the south coast of Hudson Strait close to the edge of Ungava Bay (**Figure 6b**). Thus, this group of stations was identified as the Coastal-Hudson (CH) assemblage. Cirripedia were found at all of the CH stations and were the most abundant taxon, representing about 56% of the total zooplankton abundance (122 ± 187 x10^3 ind m^{-2}). *Pseudocalanus* spp. comprised the second most abundant taxon, contributing 13% of the CH zooplankton composition. Cirripedia was the main contributing taxon to the differentiation of the CH group (SIMPER analysis; **Table 3**).

The remaining 389 stations further separated into two groups at the 49% similarity level (**Figure 6a**). The geographic coverage by the 278 stations of the first of these groups was almost continuous over the study region. This group extended from the slope of the northern Chukchi Sea, through the Canada Basin and offshore sector of the Beaufort Sea, the western and eastern parts of the CAA; then in the east, from Kane Basin above 79°N to Labrador Saglek fjord below 59°N, with an expansion in the central Hudson Strait and Bay (**Figure 6b**). This group was identified as the Arctic-oceanic (AOc) assemblage. It was dominated by the copepods *Oithona similis*, *Pseudocalanus* spp., *Triconia borealis*, *Microcalanus* spp., *Metridia longa*, *Calanus glacialis* and *C. hyperboreus*, which, together, represented 86% of the numerical composition (**Table 2**), totalling 133 ± 179 x10^3 ind m^{-2}.

The last group comprised 111 stations in 10 clusters scattered across the study region: 4 coastal stations in the northeast Chukchi Sea, 3 stations on the Mackenzie Shelf, 49 stations in the South Kitikmeot, 6 stations in a shoaling section of the Northwest Passage between Viscount Melville Sound and Barrow Strait, 1 station <170 m in depth close to Ellesmere Island on the western side of the North Water, 1 station close to Iqaluit in Frobisher Bay, 4 stations in Foxe Basin, 12 stations in Hudson Bay, 8 shallow stations along the south coast of Hudson Strait, and 23 of the 27 stations located in the four Labrador fjords (**Figure 6b**). This group was identified as the Arctic-shelf (AS) assemblage. Like the AOc assemblage, the small copepods *Pseudocalanus* spp. and *Oithona similis* dominated the zooplankton of the AS assemblage, with these two species comprising 47 and 27% of the 202 ± 283 x10^3 ind m^{-2}, respectively (**Table 2**). Ranked third and fourth in terms of abundance, the appendicularian *Fritillaria borealis* and the complex of small copepod species *Acartia* spp. comprised 7 and 3% of the zooplankton present in this assemblage. The varying proportions of the 6 major taxa of the AOc assemblage and of *Fritillaria borealis* and *Acartia* spp. were the main drivers of the differentiation between the AOc and AS assemblages (**Table 3**). In the CAA, the rather shallow areas of the South Kitikmeot and Barrow Strait, hosting essentially AS stations, were the main discontinuities in the geographic coverage of the AOc assemblage (**Figure 6b**).

From the 44 sites sampled repeatedly during the 14-year study period, 36 consistently hosted the same assemblage with zooplankton composition characteristic of either AOc or AS. These sites were in Amundsen Gulf (**Figure 9a**), the North Water (**Figure 9b**), Queen Maud Gulf in the South Kitikmeot (**Figure 9c**), Viscount Melville Sound, and Lancaster Sound. The remaining eight (18%) had zooplankton assemblages that changed or fluctuated between AOc and AS assemblages from year to year. Two of these sites were located on the shallow <45 m in depth part of the Mackenzie Shelf (**Figure 9d** and **e**), 2 sites on the northeast and northwest of Larsen Sound, respectively (**Figure 9f** and **g**), 1 site in eastern Barrow Strait (**Figure 9h**), 1 site in Nachvak (**Figure 9i**), and 2 sites in Saglek (**Figure 9j** and **k**) fjords.

The NMDS demonstrated well the partitioning of the four zooplankton assemblages in a 2-dimensional ordination with a stress value of 0.18, thus validating the cluster analysis (**Figure 10**). The AOc and AS assemblages separated essentially along the horizontal axis of the ordination. Stations of the CH assemblage, which had the lowest intra-group similarity percentage (58%; **Table 3**), were scattered mostly vertically on the left side of the ordination whereas the spread of the LS stations, with an intra-

Table 3. Taxa ranked according to their relative contribution to the multivariate intragroup similarity (%) and dissimilarities between pairs of the four main zooplankton assemblages[a]

Assemblage[a]	LS	CH	AOc	AS
LS	(76)	–	–	–
	Oithona similis (16)	–	–	–
	Microcalanus spp. (10)	–	–	–
	Calanus finmarchicus (9)	–	–	–
	Oithona atlantica (8)	–	–	–
	Oncaea spp (4)	–	–	–
	Boroecia maxima (4)	–	–	–
	Spinocalanus sp. (4)	–	–	–
	Calanus hyperboreus (4)	–	–	–
	Metridia longa (3)	–	–	–
	Scolecithricella minor (3)	–	–	–
CH	–	(58)	–	–
	Cirripedia (13)	Cirripedia (32)	–	–
	Calanus finmarchicus (7)	*Pseudocalanus* spp. (19)	–	–
	Oithona atlantica (6)	*Oithona similis* (14)	–	–
	Pseudocalanus spp. (6)	*Triconia borealis* (11)	–	–
	Oithona similis (5)	*Microcalanus* spp. (8)	–	–
	Microcalanus spp. (4)	Polychaeta (4)	–	–
	Triconia borealis (3)	*Acartia* spp. (2)	–	–
	Oncaea spp. (3)	*Calanus glacialis*[b] (2)	–	–
	Spinocalanus sp. (3)	–	–	–
	Boroecia maxima (3)	–	–	–
AOc	–	–	(60)	–
	Calanus finmarchicus (8)	Cirripedia (18)	*Oithona similis* (23)	–
	Oithona atlantica (7)	*Oithona similis* (8)	*Pseudocalanus* spp. (14)	–
	Pseudocalanus spp. (6)	*Metridia longa* (6)	*Microcalanus* spp. (12)	–
	Triconia borealis (4)	*Microcalanus* spp. (5)	*Triconia borealis* (11)	–
	Oncaea spp. (3)	*Triconia borealis* (5)	*Metridia longa* (8)	–
	Spinocalanus sp. (3)	*Pseudocalanus* spp. (5)	*Calanus glacialis*[b] (7)	–
	Metridia longa (3)	*Calanus hyperboreus* (4)	*Calanus hyperboreus* (6)	–
	Microcalanus spp. (3)	*Calanus glacialis*[b] (4)	*Limacina helicina* (2)	–
	Oithona similis (3)	*Acartia* spp. (4)	*Oncaea notopus* (2)	–
	Calanus glacialis[b] (2)	Euphausiidae (3)	*Oikopleura vanhoeffeni* (2)	–
AS	–	–	–	(63)
	Pseudocalanus spp. (13)	Cirripedia (20)	*Pseudocalanus* spp. (12)	*Pseudocalanus* spp. (39)
	Calanus finmarchicus (7)	*Pseudocalanus* spp. (12)	*Microcalanus* spp. (8)	*Oithona similis* (23)
	Oithona atlantica (6)	*Oithona similis* (7)	*Triconia borealis* (7)	*Fritillaria borealis* (7)
	Microcalanus spp. (6)	*Fritillaria borealis* (7)	*Fritillaria borealis* (7)	*Calanus glacialis*[b] (7)
	Fritillaria borealis (4)	*Triconia borealis* (7)	*Metridia longa* (6)	*Acartia* spp. (4)

(continued)

Table 3. *(continued)*

Assemblage[a]	LS	CH	AOc	AS
	Oncaea spp. (3)	*Acartia* spp. (5)	*Oithona similis* (6)	*Triconia borealis* (3)
	Oithona similis (3)	*Microcalanus* spp. (4)	*Acartia* spp. (4)	*Microcalanus* spp. (3)
	Spinocalanus sp. (3)	Euphausiidae (4)	*Calanus hyperboreus* (4)	*Parasagitta elegans* (2)
	Boroecia maxima (3)	*Calanus glacialis*[b] (4)	*Calanus glacialis*[b] (3)	*Oïkopleura vanhoeffeni* (2)
	Acartia spp. (3)	Bivalvia (3)	*Oncaea notopus* (3)	*Limacina helicina* (2)

[a]Defined by cluster analysis (**Figure 6**) and designated Labrador Sea (LS), Coastal-Hudson (CH), Arctic-oceanic (AOc), and Arctic-shelf (AS) zooplankton assemblages.

[b]*Calanus glacialis* and *C. marshallae* pooled.

group similarity percentage of 76%, was limited to the top-right of the ordination (**Figure 10**).

Environmental variables underpinning the geographical distribution of zooplankton

The multiple regression analysis revealed highly significant relationships ($p < 0.001$) between 11 of the 15 environmental variables considered and the scores of the 2-dimensional NMDS ordination summarizing the mesozooplankton community structure (**Table 4**). Water-column mean salinity explained 43% of the variance in the zooplankton composition among the 409 stations, followed by station depth which explained 39% of the variance. Those two environmental variables were well correlated (Spearman $r_s = 0.83$, $p < 0.001$; Table S3) and weighted most in the separation of the AOc and AS assemblages, as illustrated by the small angles with the horizontal axis of the ordination (**Figure 10**). Latitude accounted for 26% of the variance. However, this variable operated along an axis that was at a greater angle with the main axis of separation than the angles produced from the direction cosines of mean salinity and station depth. The other eight environmental variables showing a highly significant relationship with the scores of the NMDS, namely: water column average temperature, chlorophyll fluorescence, day of sampling, surface (0–10 m) mean temperature, surface mean salinity, the ice-free season between ice breakup and freeze-up, mean annual surface Chl-a, the summer ice-free period (<50% ice cover) prior to sampling, explained more modest amounts (5–14%) of the variance. Although significant, the contribution of the depth-of-fluorescence maximum to the variance in zooplankton composition did not exceed 3%.

The "BEST" procedure in PRIMER6, identified these four environmental variables: water-column salinity, station depth, latitude, and water-column temperature, as the best combination to explain the multivariate patterns of zooplankton community composition (Spearman's rank correlation $\rho s = 0.554$; **Table 5**). The correlation between the biotic patterns and water-column salinity alone was $\rho s = 0.381$, whereas correlations of 0.364, 0.300, and 0.258 were found with station depth, water column temperature, and latitude, respectively.

The LS assemblage was found in deeper areas than the other assemblages (Kruskal-Wallis $p < 0.001$), with a mean depth of 1445 ± 747 m, compared to 478 ± 509, 100 ± 53, and 77 ± 47 m for AOc, AS, and CH, respectively (Kruskal-Wallis $p < 0.001$). Mean depths of the latter two shallower groups did not differ significantly from each other. The AOc stations showed an extensive depth range of 30–3860 m. However, only 40 of these 278 stations had depths shallower than 150 m. The most southeastern and deepest LS group, which had a thicker layer of Atlantic Water due to a station depth range of 510–2485 m, showed a higher water-column salinity (34.48 ± 0.24) than the other groups (Kruskal-Wallis $p < 0.001$). This variable was also higher at the AOc stations (32.93 ± 1.30) than in the CH and AS groups, which had respective salinities of 31.65 ± 1.11 and 30.31 ± 2.25. Mean latitude of AOc stations was higher than those of the other groups (70.87 ± 4.89 versus <66°N; Kruskal-Wallis $p < 0.001$). All of the LS and CH stations were below the Arctic Circle.

At the species level, abundance correlated with water-column salinity for 13 of the 18 taxa that comprised >90% of the total zooplankton numerical composition, except for *Oithona similis*, *Calanus glacialis*, *Oikopleura vanhoeffeni*, *Limacina helicina*, and the Bivalvia meroplankton (**Table 6**). This correlation was negative only for the neritic *Pseudocalanus* spp., *Acartia* spp., *Fritillaria borealis*, and Cirripedia meroplankton. Similarly, abundance correlated negatively with station depth for the latter four taxa, whereas the correlation was positive for 12 of the dominant taxa. The abundance of *Pseudocalanus* spp., *Acartia* spp., and *Oithona atlantica* decreased with increasing latitude, whereas the relationship was positive for 9 taxa. On the other hand, *C. hyperboreus* and Cirripedia were the only taxa for which abundance decreased with the increase of the ice-free period before sampling. There was no or only weak correlation between this variable and the abundance of 11 of the main taxa. Cirripedia abundance increased with surface Chl-a concentration averaged over the sampling year, while no significant correlation was found between this variable and the abundance of most taxa, including known herbivores such as *Calanus* spp. The correlation was even negative for the complex of mainly herbivorous *Pseudocalanus* species and for the

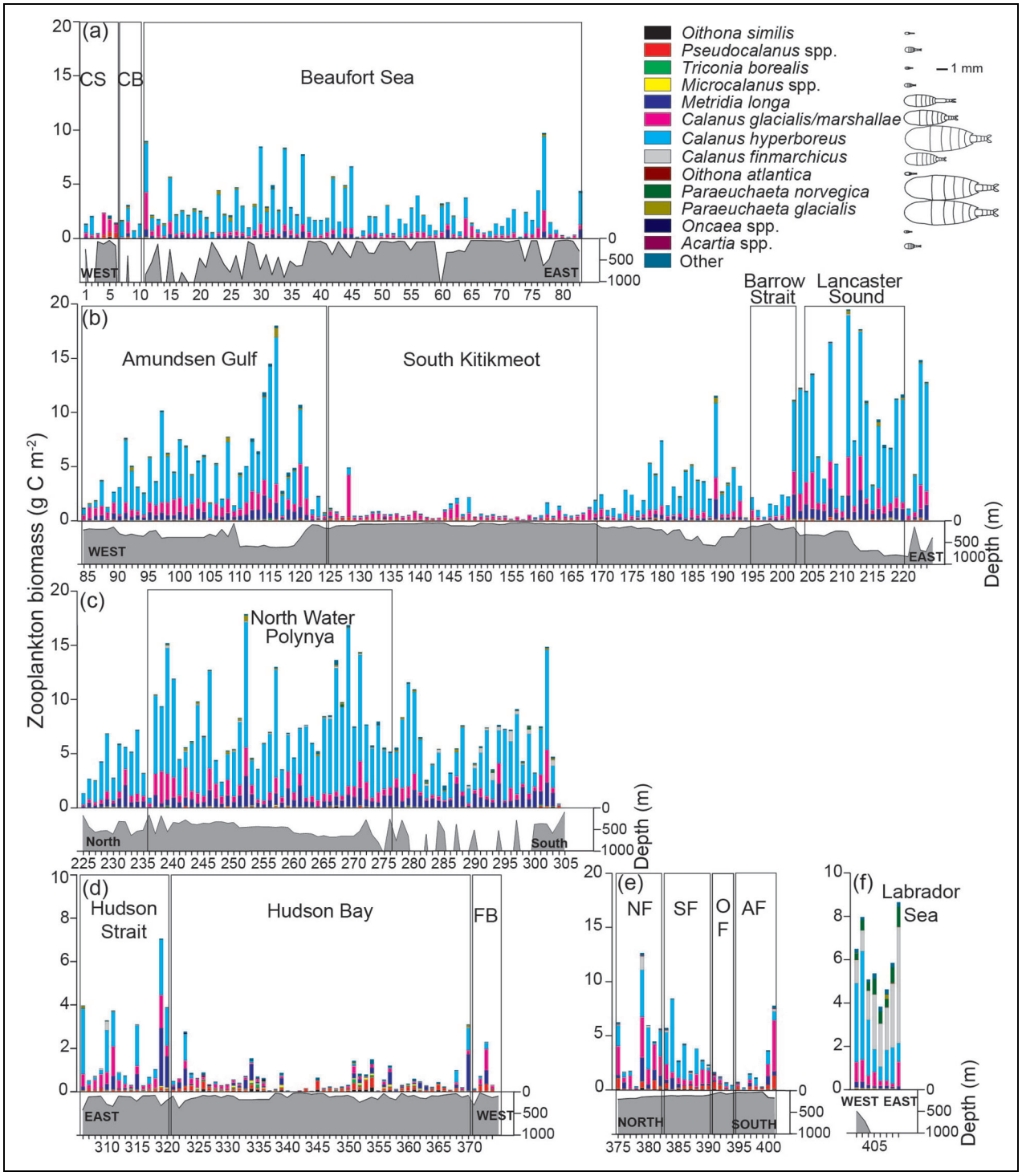

Figure 7. Contribution of main taxa to water-column integrated copepod biomass in the North American Arctic. The 409 stations sampled in the Western Arctic, including (a) the Chukchi Sea (CS), Canada Basin (CB), and Beaufort Sea; (b) the Canadian Arctic Archipelago from Amundsen Gulf and South Kitikmeot to Barrow Strait and Lancaster Sound; (c) Baffin Bay from north to south; (d) the Hudson complex comprising Hudson Strait, Hudson Bay, and Foxe Basin (FB); (e) Labrador fjords, including Nachvak (NF), Saglek (SF), Okak (OF), and Anaktalak fjords (AF); and (f) the Labrador Sea, superimposed on the bathymetry of the respective regions of the American Arctic and Subarctic. Note the different scales of the biomass axis for the Hudson complex and Labrador Sea.

omnivores *Oithona similis*, *Oncaea* spp., *Oikopleura vanhoeffeni*, and *Limacina helicina*. The abundance of the herbivore *C. hyperboreus*, the omnivores *Metridia longa*, *Microcalanus* spp., *Triconia borealis* and other oncaeids, *O. similis*, and the carnivores *Paraeuchaeta norvegica* and *P. glacialis* decreased with increasing water-column fluorescence; only the abundance of *Pseudocalanus* spp. and Cirripedia larvae increased with this variable.

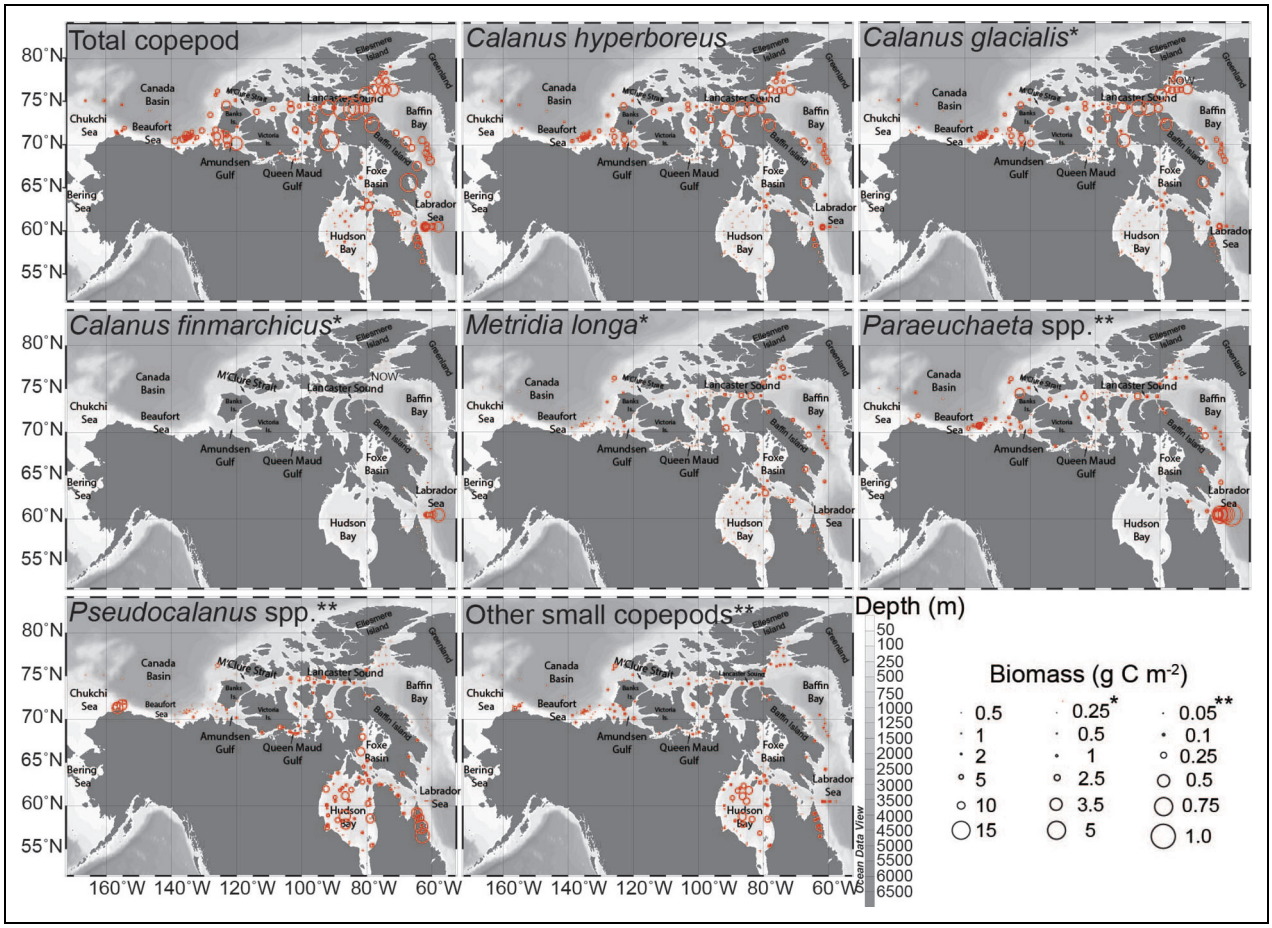

Figure 8. Geographic distribution of the water-column integrated biomass of total copepod and dominant copepod taxa. Biomass averaged over the sampling years 2005–2018 for the 283 ArcticNet sampling sites across the North American Arctic and eastern Subarctic. Note the lower scales (indicated by asterisks and correspondingly altered symbol sizes) for *Calanus glacialis*, *C. finmarchicus*, and *Metridia longa*, and also for *Paraeuchaeta* spp., *Pseudocalanus* spp., and other small copepods (summing the biomass of *Acartia* spp., *Microcalanus* spp., *Oithona atlantica*, *O. similis*, *Oncaea* spp., and *Triconia borealis*).

Discussion

Biogeography of zooplankton assemblages in the North American Arctic

This study offers novel insights into the mechanisms controlling zooplankton biogeography across a vast expanse of the North American Arctic and eastern Subarctic where we identified four main assemblages: (1) Arctic-oceanic, (2) Arctic-shelf, (3) Coastal-Hudson, and (4) Labrador Sea. Until now, zooplankton biogeographic patterns on such a continental scale have only been described by Pomerleau et al. (2011; 2014). Their two studies were based on results from an incomplete sampling of the water column limited in depth to the top 0–100 m, which showed that zooplankton composition in the epipelagic zone varied mainly with temperature and salinity in that surface layer. Our investigation, backed by a full water column-integrated sampling, revealed that water-column salinity and station depth explained best the zooplankton assemblage differentiation in this topographically complex part of the Arctic (station depth range of 26–3860 m; **Figure 1**). Nevertheless, salinity most likely had no direct effect on zooplankton biology and composition, as the depth-averaged range of measured salinities of 24.16–34.44 was comparable to the range of salinities of 20–34 suitable for the dominant Arctic zooplankton taxa (see figure 5 of Grainger, 1965). Water-column salinity was in fact a strong correlate of station depth (Table S3). The latter defines the presence or absence of the main subsurface water masses, the Polar Halocline and the more saline Atlantic Water, the thickness of which correlates with depth-averaged salinity. Thus, the link between zooplankton biogeography and water-mass features is not as straightforward to establish for the whole water-column assemblage as when only the epipelagic zone was considered.

Combined with hydrographic and zooplankton ecological knowledge, the geographic distribution of the assemblages illustrated in **Figure 6** suggests that a complex interplay between zooplankton habitat preference, vertical distribution, and topographic features affecting ocean circulation influences the observed large-scale zooplankton community structure. The extensive geographic distribution of the Arctic-oceanic and Arctic-shelf assemblages is congruent with the general eastward direction of the

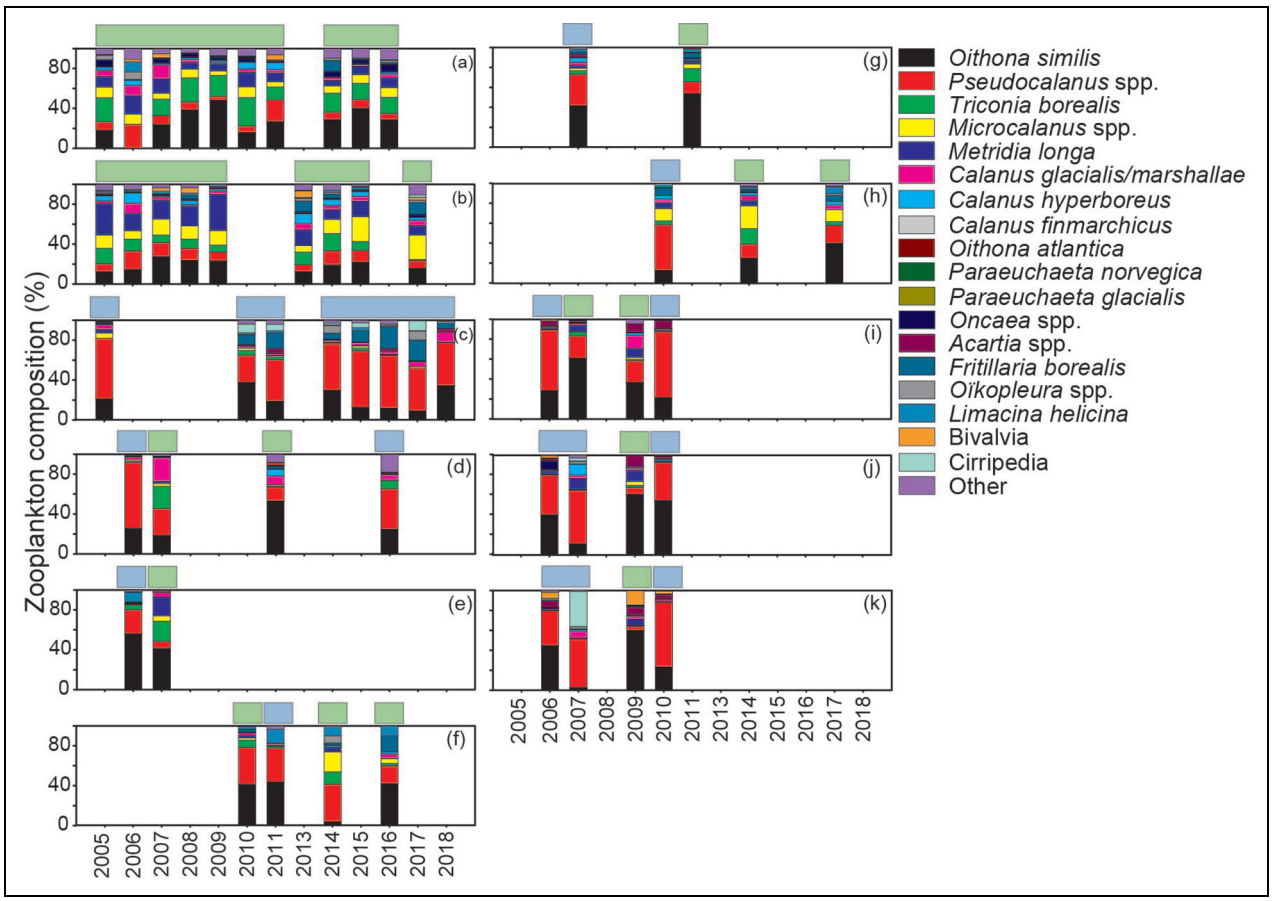

Figure 9. Interannual variations in mesozooplankton numerical composition at selected sites across the North American Arctic. Sites in (a) Amundsen Gulf, (b) the North Water Polynya, (c) Queen Maud Gulf, (d, e) Mackenzie Shelf, (f) northeast of Larsen Sound, (g) northwest of Larsen Sound, (h) eastern Barrow Strait, (i) Nachvak Labrador fjord, and (j, k) Saglek Labrador fjord. Zooplankton taxonomic compositions typical of Arctic-oceanic (AOc) and Arctic-shelf (AS) assemblages, as defined by cluster analysis (**Figure 6**), are indicated by horizontal green and blue bars, respectively, above each panel.

ocean flow from the northwestern boundary of the study region, through the CAA, and then southward along the eastern Canadian coastline with the Baffin Island and Labrador currents (**Figure 1a**). The Arctic-oceanic assemblage shared broad similarities with communities in offshore slope and basin zones >200 m in depth of the Eastern and Western Arctic (Kosobokova et al., 1997; Hopcroft et al., 2005) and polynya systems, including the Cape Bathurst (Darnis et al., 2008), North Water, and Eastern Lancaster Sound polynyas (Ringuette et al., 2002). The distinctive species of these Arctic-oceanic communities, *Triconia borealis*, *Microcalanus* spp., and *Metridia longa*, and the long-range seasonal and vertically migrating *Calanus hyperboreus* and *C. glacialis* are known to spend most of their time in the mesopelagic Atlantic Water layer below 200 m (Auel and Hagen, 2002; Darnis and Fortier, 2014).

Areas shallower than 200 m in depth do not include deep habitats needed by some mesopelagic species. This aspect partly explains why the Arctic-shelf zooplankton composition, dominated by the neritic *Pseudocalanus* spp., *Acartia* spp., and *Fritillaria borealis*, was typical of assemblages found in the shelf areas of the Laptev Sea (Kosobokova et al., 1997), Beaufort Sea (Darnis et al., 2008; Smoot and Hopcroft, 2016), and Barrow Strait (Fortier et al., 2002). Furthermore, several sills <150 m in depth across the CAA (**Figure 1a**) block the flow of the underlying Atlantic Water and, thus, would limit the transport of mesopelagic zooplankton and seasonal vertical migrators downstream of these barriers. The shallow Queen Maud Gulf, located between two sills <30 m deep and with a maximum depth of <120 m, exemplifies such a setting and has been identified as a potential barrier to dispersal of pelagic fish populations (Bouchard et al., 2018). This potential barrier appears to be particularly true for the forage species Arctic cod (*Boreogadus saida*), which is scarce in the Queen Maud Gulf. Barrow Strait and Foxe Basin are other shallow areas downstream of sills restricting the distributional range of oceanic zooplankton within the CAA. Contrary to Foxe Basin, the deeper Hudson Strait, devoid of sills, presented no obstacle to the expansion of the Arctic-oceanic assemblage into central and western Hudson Bay.

The constancy in zooplankton composition at most of the 44 sites sampled multiple times during the 14-year study period indicates that the overall geographic

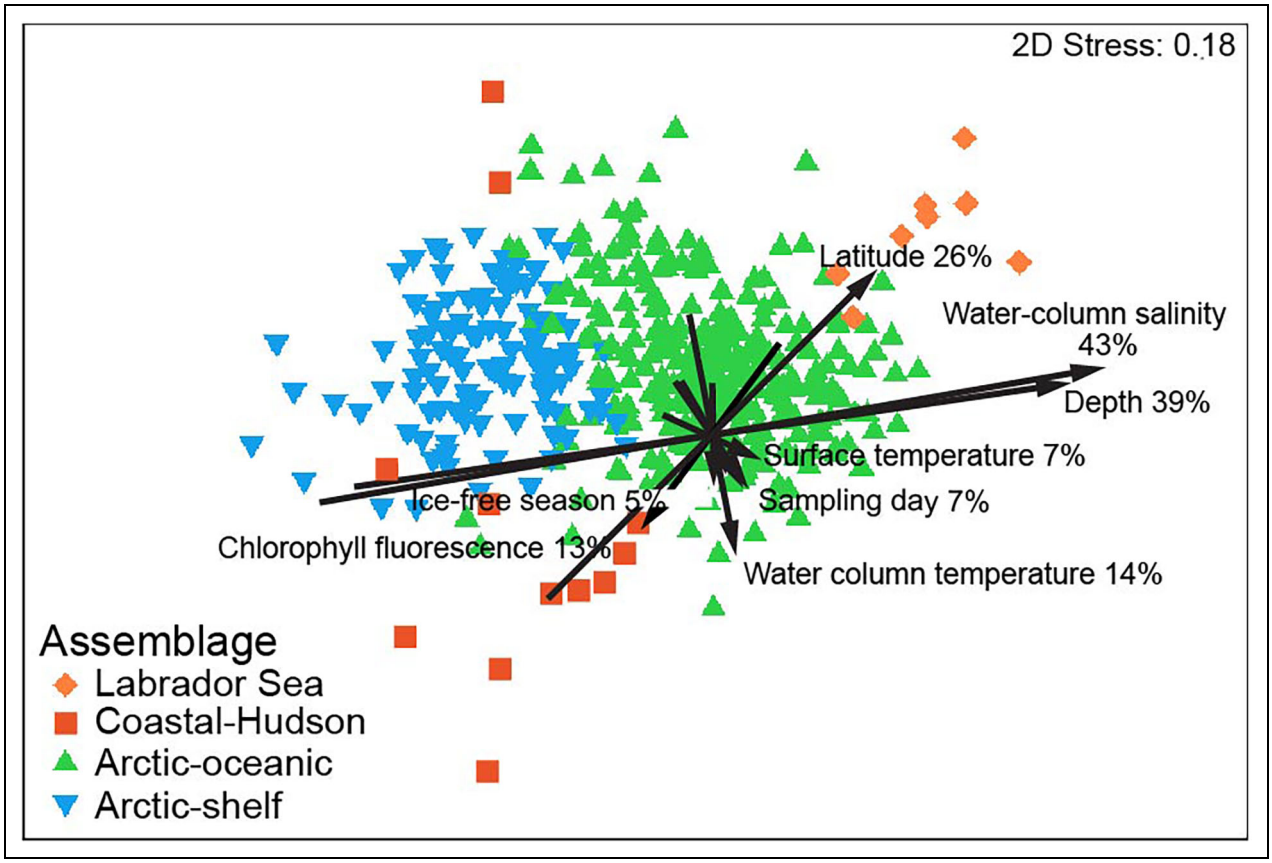

Figure 10. Non-metric multidimensional scaling ordination plotting stations based on zooplankton composition similarities. Significant multiple regression lines between environmental variables and NMDS scores shown with the percentage of variance in zooplankton composition explained by an environmental variable. Groups of stations comprising each of the four main zooplankton assemblages (color-coded for Labrador Sea, Coastal-Hudson, Arctic-oceanic, and Arctic-shelf) are identified in **Figure 6**.

distribution of the Arctic-oceanic and Arctic-shelf assemblages is consistent (**Figure 9**). Six of the 8 sites experiencing interannual shifts in zooplankton composition, from Arctic-shelf to Arctic-oceanic assemblages, match locations with known oceanographic features amplifying upwelling events and episodic rise of underlying water masses to the surface, as seen on the Mackenzie Shelf of the Beaufort Sea (Carmack and Chapman, 2003; Wang et al., 2012). The 2 remaining sites were in the northern Labrador Nachvak and Saglek fjords, the oceanography of which is poorly documented (Brown et al., 2012). Thus, upwelling over the Mackenzie Shelf and shoal areas in the southeastern M'Clintock Channel and Larsen Sound, and the west side of Barrow Strait, could occasionally transport oceanic zooplankton over these shallow transition areas.

The scarcity of the North Pacific copepods *Metridia pacifica*, *Neocalanus* spp. and *Eucalanus* spp. prevented a Pacific characterization of zooplankton composition in the Chukchi Sea-Canada Basin area. This observation is consistent with previous studies indicating that the zooplankton communities of the North American Arctic above 70°N and east of 170°W (our westernmost study boundary) are so far only marginally influenced by North Pacific taxa advected through Bering Strait (Nelson et al., 2009; Pomerleau et al., 2014; Ershova et al., 2015; Matsuno et al., 2015; Smoot and Hopcroft, 2016). By contrast, the Labrador Sea zooplankton assemblage on the subarctic eastern side of the study area had a strong Atlantic identity provided by the high share of the North Atlantic copepods *Calanus finmarchicus*, *Oithona atlantica*, and mesopelagic taxa indicative of the Atlantic Water layer (Kosobokova et al., 1997; Auel and Hagen, 2002). The mix of Atlantic and Arctic species in this deep sector of the Labrador Sea results from the confluence of the cold southward-flowing Labrador Current and a minor westward-flowing branch of the Atlantic-influenced West Greenland Current (**Figure 1a**). The low representation of the Atlantic expatriates *C. finmarchicus* and *O. atlantica* in the samples collected north of Davis Strait failed to confer an Atlantic identity on the zooplankton assemblage in southwestern Baffin Bay. This observation contrasts with the current situation on the eastern side of Baffin Bay near Disko Island, Greenland, where a shift in dominance of the *Calanus* complex has been occurring in favour of the boreal *C. finmarchicus* over the last decades (Møller and Nielsen, 2020). Our sampling did not include areas north of the Arctic Circle under a measurable influence of the West Greenland Current. We conclude that the zooplankton biogeography in the North American Arctic is so far not structured according to a Pacific-Atlantic longitudinal

Table 4. Relationships between environmental variables and the scores of stations on the first and second axes of the NMDS ordination (Figure 10)

	Regression Weights[a]				
Environmental Variable	**First Axis**	**Second Axis**	r^{2b}	F^c	p^d
Water-column salinity	0.994	−0.111	0.43	153.13	<0.001
Station depth	0.998	−0.057	0.39	131.85	<0.001
Latitude	0.706	−0.708	0.26	70.01	<0.001
Water-column temperature	−0.190	0.982	0.14	31.56	<0.001
Chlorophyll fluorescence	−0.596	−0.803	0.13	21.76	<0.001
Day of sampling	−0.551	0.834	0.07	15.59	<0.001
Surface (0–10 m) average temperature	−0.755	0.655	0.07	14.64	<0.001
Surface (0–10 m) average salinity	0.972	0.231	0.06	12.75	<0.001
Season with <50% ice cover	−0.446	0.895	0.06	12.14	<0.001
Mean annual surface Chl-a	0.037	0.999	0.06	11.12	<0.001
Period with <50% ice prior to sampling	−0.301	0.953	0.05	9.58	<0.001
Depth of fluorescence maximum	0.704	−0.709	0.03	6.58	0.02
Day when ice concentration <50%	−3.407	−4.491	0.01	2.80	ns[d]
Year of sampling	−0.001	−0.148	<0.01	2.16	ns
Longitude	−0.390	2.452	<0.01	0.35	ns

[a]Regression weights of multiple regression analysis from equation of Kruskal and Wish (1978).

[b]Adjusted coefficient of determination measuring the proportion of the variance explained by the linear model.

[c]Value of the statistical F-test.

[d]ANOVA p values; ns = not significant.

Table 5. Correlations[a] between environmental variables and mesozooplankton community structure

K	ρs	Environmental Variable
1	0.381	Water-column salinity
1	0.364	Station depth
1	0.300	Latitude
1	0.258	Water-column temperature
2	0.483	Water-column salinity + latitude
3	0.531	Water-column salinity + station depth + latitude
4	0.554	Water-column salinity + station depth + latitude + water-column temperature

[a]BEST/BIO-ENV analysis in PRIMER V6 revealing combinations of K variables that deliver highest Spearman's rank correlations (ρs) between a mesozooplankton assemblage similarity matrix and resemblance matrices generated from different subsets of a matrix made of a suite of environmental variables.

gradient, but rather by a bathymetric gradient when all the pelagic habitats from the surface to the bottom are considered.

The use of a large ship to deploy plankton nets limited shallow-water sampling (<20-m depth) and the study of zooplankton in estuarine habitats strongly influenced by freshwater from river plumes, such as the inner Mackenzie Shelf and the coastal part of the South Kitikmeot. Thus, abundances of euryhaline taxa, including *Eurytemora* spp., *Limnocalanus* spp. and *Temora* spp. indicative of brackish-water ecosystems, were too low in our dataset to demarcate a "Plume" assemblage as previously detected in the coastal Beaufort and Laptev seas (Kosobokova et al., 1997; Walkusz et al., 2009; Smoot and Hopcroft, 2016). Furthermore, a dataset with more coastal stations certainly would have enabled a more precise delimitation of the habitats of the Arctic-shelf assemblage.

Depth and differences in zooplankton biodiversity and biomass distribution

The water column in the deeper areas of the North American Arctic and Labrador slope comprises several water masses of various origins, providing multiple habitats for a diverse group of pelagic-oceanic organisms, compared to the less complex hydrographic setting at shallow depths. Hence, the Labrador Sea and Arctic-oceanic assemblages, found in water columns hundreds of metres thick, displayed higher biodiversity indices than the shallow-water Arctic-shelf and Coastal-Hudson assemblages (**Table 1**). Moreover, the discrepancy between deep- and shallow-water assemblages in the abundances of the Arctic copepods *Calanus hyperboreus*, *C. glacialis* and *Metridia longa*

Table 6. Spearman's rank correlation coefficients (ρρs) between environmental variables and abundance of dominant zooplankton taxa in the North American Arctic

Taxon	Water-Column Salinity	Station Depth	Latitude	Ice-Free Season	Annual Surface Chl-a	Water-Column Fluorescence
Oithona similis	0.080	0.167**	−0.076	0.288***	−0.145*	−0.197**
Pseudocalanus spp.	−0.428***	−0.367***	−0.294***	0.153*	−0.140*	0.224***
Triconia borealis	0.396***	0.450***	0.303***	0.157*	−0.061	−0.227***
Microcalanus spp.	0.540***	0.645***	0.284***	−0.092	−0.099	−0.355***
Metridia longa	0.614***	0.733***	0.464***	0.289***	−0.065	−0.351***
Calanus glacialis	0.074	0.202***	0.347***	0.368***	−0.054	−0.081
Calanus hyperboreus	0.556***	0.649***	0.577***	−0.244***	0.022	−0.380***
Calanus finmarchicus	0.267***	0.293***	−0.048	0.054	0.085	−0.072
Oithona atlantica	0.266***	0.223***	−0.187**	−0.103*	0.030	−0.179*
Paraeuchaeta norvegica	0.332***	0.295***	−0.048	−0.012	0.052	−0.252***
Paraeuchaeta glacialis	0.369***	0.459***	0.504***	0.168**	−0.075	−0.184*
Oncaea sp.	0.614***	0.679***	0.375***	0.021	−0.136*	−0.339***
Acartia spp.	−0.475***	−0.484***	−0.476***	0.128*	−0.027	0.243***
Fritillaria borealis	−0.245***	−0.209***	0.081	0.027	−0.043	−0.071
Oikopleura spp.	−0.093	0.079	0.356***	0.074	−0.145*	−0.036
Limacina helicina	0.052	0.160**	0.337***	0.102*	−0.117*	−0.021
Bivalvia	−0.078	−0.057	0.207***	0.590***	0.080	0.057
Cirripedia	−0.121*	−0.203***	−0.050	−0.168**	0.222***	0.239***

*ρ < 0.05. **ρ < 0.001. ***ρ < 0.0001.

and the boreal *C. finmarchicus* led to a spatial distribution of mesozooplankton biomass largely skewed towards the deep areas within the CAA, Baffin Bay, and Labrador Sea (**Figure 8**). The sum of abundances of these large copepods, representing 80% of copepod biomass in the entire study area, was 5 times higher in the deep-water assemblages (25.6 ± 5.2 x10^3 ind m^{-2}; **Table 2**) than in the shallow-water ones (5.3 ± 4.8 x10^3 ind m^{-2}). Consequently, the mean biomass in the two deep-water assemblages (5.2 ± 0.7 g C m^{-2}) was approximately 6 times higher than in the shallow-water ones (0.9 ± 0.9 g C m^{-2}). In the shallow shelf areas, the *Calanus* species remained dominant in terms of biomass, though to a much lesser extent, despite a lower contribution to total abundance compared to the deep areas. This biomass dominance was essentially due to the much larger size of the *Calanus* species than the numerically dominant neritic copepods, including *Pseudocalanus* spp. Nevertheless, the hotspots of copepod biomass identified in the central Amundsen Gulf, eastern Lancaster Sound, the North Water, and Baffin Bay were in waters >350 m in depth, and all were occupied by the Arctic-oceanic assemblage (**Figures 6** and **8**).

Our estimates compared well with those by previous studies in the same areas (Table S4), indicating that the skewness risk due to the spatially uneven sampling effort is low for our mapping of copepod biomass. Biomass values above 7 g C m^{-2} were only observed in these North American Arctic hotspots and on the opposite side of the Arctic in Rijpfjord, Svalbard, in August 2010 (Hop et al., 2019). Considering only copepods leads to a conservative estimate of mesozooplankton biomass that could be biased if the copepod fraction constituted only a minor part of the assemblage. However, copepods account generally for >80% of mesozooplankton biomass in shelf, slope, and basin areas of the North American Arctic (Hopcroft et al., 2005; Darnis et al., 2008; Smoot and Hopcroft, 2016), supporting a consistent description of mesozooplankton biomass patterns solely based on copepods.

Primary production, sea ice, water chemistry, and differences in zooplankton assemblages

Food availability is a key driver of zooplankton geographic distribution (Druon et al., 2019). A main strategy among the dominant Arctic zooplankton is to take advantage of the intense pulse of biological productivity in spring–summer to fuel metabolic needs for reproduction, growth, development, and lipid storage for overwintering (Falk-Petersen et al., 2009). However, the proxies of algal biomass used in our analyses, namely the mean annual surface Chl-a and chlorophyll fluorescence at the time of sampling, only explained a small fraction of the variance in zooplankton composition (6 and 13%, respectively). Ocean color remote sensing provides time series, enabling

the temporal integration of Chl-a over the ice-free productive season, but technical limitations affect calculations of Chl-a concentration and pelagic primary production at high latitudes (Babin et al., 2015). Sea ice and frequent clouds prevent the estimation of sea-ice algae and under-ice phytoplankton production in the early stages of the productive season, a crucial period for the arctic *Calanus* species (Søreide et al., 2010; Darnis et al., 2019). Additionally, the satellite sensors cannot reach the subsurface chlorophyll maxima following the deepening nutricline as surface nutrients get depleted through the ice-free season in highly stratified seas. These constraints may lead to underestimation of Chl-a biomass. Heavy loading of colored dissolved organic matter in river plumes can cause Chl-a overestimation in coastal waters of the Mackenzie Shelf, South Kitikmeot, and Hudson Bay (**Figure 4**). Our satellite-based estimates of surface Chl-a concentration, averaged over the ice-free period, therefore may not be illustrative of the real food availability to zooplankton. The absence of correlation between this variable and the abundance of a large majority of the dominant zooplankton herbivores and omnivores (**Table 6**) supports this hypothesis. Furthermore, the non-motile algae, mainly concentrated in the epipelagic layer, may be subject to different advective forces than the zooplankton, most of which are able to swim vertically and influence their dispersal. The assessment of annual Chl-a at a stationary site makes the investigation of the algae-zooplankton trophic relationship even more complex because the captured zooplankton grew from feeding during months while being transported with currents in a Lagrangian system. The snapshot of mean water-column chlorophyll fluorescence at sampling is also unlikely to be representative of food availability during the weeks prior to sampling (Darnis et al., 2008).

The ice-free season, a rough proxy of the length of the pelagic primary production season, notwithstanding nutrient constraints, was also not a good determining variable of zooplankton community patterns at such a large spatial scale. However, comparing maps of copepod biomass (**Figure 8**) and of polynyas and flaw leads (Niemi et al., 2019) shows that the main hotspots of biomass were near or in polynyas, such as the North Water, Lancaster Sound, and Cape Bathurst polynyas. A good correspondence between the geographic distribution of zooplankton biomass and of phytoplankton biomass and production was also described by Ardyna et al. (2011). They identified two main phytoplankton assemblages in the Canadian High Arctic: one characterized mainly by pico-flagellate cells and low biomass of diatoms in the southeastern Beaufort Sea and central CAA, and the other characterized by larger diatom cells in the nano- and micro-phytoplankton size class distributed in the centre of Amundsen Gulf, Lancaster Sound, and Northern Baffin Bay. The zooplankton biomass hotspots, where the herbivores *Calanus hyperboreus*, *C. glacialis*, and the omnivore *Metridia longa* dominated, were all associated with the diatom-based food web.

Low seawater pH has been shown to cause mortality or reduce long-term fitness of abundant arctic copepods such as the coastal *Acartia longiremis* and *Calanus glacialis* (Thor et al., 2018; Halsband et al., 2021) and calcifying zooplankton with a calcium carbonate shell made of aragonite, such as the pteropod *Limacina helicina* (Niemi et al., 2021). Thus, variability in seawater carbonate chemistry could influence zooplankton geographic distribution. Yet, no clear pattern emerged when comparing the distribution of zooplankton communities with surface seawater pH and saturation state with respect to the carbonate mineral aragonite described by Beaupré-Laperrière et al. (2020). The Canada Basin and Queen Maud Gulf, which exhibited the lowest surface pH and undersaturation of aragonite, hosted different assemblages (Arctic-oceanic and Arctic-shelf, respectively). The lack of resolution in zooplankton vertical distribution in our study may mask the effect of a low-pH environmental stressor on zooplankton composition.

Zooplankton distribution, food web processes, and marine ecosystem management

This new large-scale spatial perspective on mesozooplankton biodiversity and biomass has applications for research on the trophodynamics, ecological connectivity, and regulation of marine ecosystem processes over a vast sector of the Arctic (Pendleton et al., 2020). A comparison of our distribution maps with previous descriptions of continental-scale distribution of marine vertebrates provides insightful information about the linkages between zooplankton and higher trophic levels. The North Water, Lancaster Sound, and Amundsen Gulf hotspots of copepod biomass (**Figure 8**) matched the locations of high acoustic backscatter (proxy of fish biomass) caused primarily by the presence of Arctic cod juveniles in the top 100 m (figure 5 of Bouchard et al., 2018). On the other hand, the South-Kitikmeot area displayed both low zooplankton biomass and fish backscatter. South of the Arctic Circle, no updated data on fish distribution was available for comparison in Hudson Bay, another shallow-water system characterized by low zooplankton biomass. Nevertheless, this region does not sustain fish stocks enabling commercial fisheries (Tremblay et al., 2019). These comparisons of distributions suggest a positive correlation between zooplankton and fish biomass in the North American Arctic and boreal regions influenced by arctic waters.

The zooplankton-fish relationship is undeniably more complex than simply one of causality. As discussed, the same topographic barrier could restrict oceanic zooplankton transport and the movement of Arctic cod and mesopelagic fish over the South Kitikmeot, as these fish tend to avoid unfavorable epipelagic habitats. Moreover, the low biomass of the large-sized and lipid-rich *Calanus* species, an important prey of pre-adult and adult arctic pelagic fish, may constrain fish population growth in this part of the CAA. On the other hand, the high abundance of small-sized zooplankton likely provides plenty of prey for fish larvae and juveniles, which prey size is restricted by their mouth gape (Bouchard and Fortier, 2020). Ichthyoplankton sampling over several years revealed the establishment of the invasive Pacific sand lance (*Ammodytes hexapterus*) in Queen Maud Gulf on its eastward range expansion in the CAA (Falardeau et al., 2017).

Furthermore, there is an Arctic char (*Salvelinus alpinus*) commercial fishery based on a large stock in this region. The anadromous chars spend the spring–summer period near shore preying on small marine fish and zooplankton. The ship's draft did not allow sampling in the shallow seasonal foraging range of Arctic char, nor did the 200-µm mesh vertical net tows target efficiently the crustacean prey of this salmonid, which are mostly neritic amphipods, euphausiids, and mysids belonging to the macrozooplankton size class (Ulrich and Tallman, 2021). As little is known about these organisms, research effort is needed to extend our results by including macrozooplankton species, which are essential for the marine food webs of the Arctic coastal areas.

So far, knowledge gaps about the geographic distribution of planktivorous long-range seasonal migrators, such as the Bowhead whale (*Balaena mysticetus*) and various seabird species (Ulrich and Tallman, 2021), complicates the analysis of trophic interactions between vertebrate predators and their zooplankton prey. Still, superimposing our zooplankton and bowhead whale distribution maps (Baird and Bickham, 2021; Hamilton et al., 2022) shows that the areas of high summer density of whales overlap with hotspots of zooplankton biomass in Amundsen Gulf and the south of Lancaster Sound (Figure S3). However, a known area of whale aggregation in the northwestern Hudson Bay does not concur with our mapping of high zooplankton biomass. Again, this discrepancy might be due to our difficulty to assess zooplankton biomass in shallow areas. Furthermore, the mapping indicates that zooplankton diversity and biomass need to be better documented in the Gulf of Boothia, a summer refuge for a significant portion of the East Canada-West Greenland bowhead whale stock.

A comprehensive understanding of the relationship between the geographic distribution of zooplankton and their vertebrate predators will also depend on the assessment of their fine-scale vertical distribution, which the coarse resolution provided by our plankton net sampling prevents from achieving. New high-resolution acoustic and imaging techniques can be used to improve knowledge of the foraging behaviors of zooplanktivorous fish, whales, and birds in light of zooplankton distribution (Fortune et al., 2020; Greer et al., 2020; Schmid et al., 2020). Seabird surveys from the Pacific Aleutian Islands to Newfoundland across the Northwest Passage revealed, again, Lancaster Sound as a hotspot of planktivorous birds in the Canadian Arctic (Wong et al., 2014). The North Water Polynya between Ellesmere Island and Greenland hosts the world's largest breeding colony of the zooplanktivore Dovekie (*Alle alle*; Figure S3), the most abundant seabird in the North Atlantic, which feeds extensively on large Arctic *Calanus* species (Møller et al., 2018). Conversely, these biogeographic studies reveal that whales and planktivorous seabirds seldom forage in the South Kitikmeot, identified in this study as a cold spot of copepod biomass.

The perimeter of most of the Marine Protected Areas and aquatic wildlife sanctuaries in the Canadian Arctic adjoins or encompasses our identified zooplankton biomass hotspots (Figure S4). The Anguniaqvia niqiqyuam Marine Protected Area, around Cape Parry in the western Canadian Arctic (Chambers and MacDonell, 2012), is just downstream of the central Amundsen Gulf hotspot, and the Tallurutiup Imanga National Marine Conservation Area (Lancaster Sound National Marine Conservation Area Feasibility Assessment Steering Committee, 2017) encompasses the Lancaster Sound hotspot. The joint Canadian-Greenlandic Inuit plan for an Indigenous Protected Area, the Pikialasorsuaq protected area, shares the location of the North Water hotspot (Pikialasorsuaq Commission, 2017). Unfortunately, we could not sample in the multi-year sea ice north of the CAA, and a literature search stressed the serious lack of knowledge on the specificities of zooplankton communities in the Tuvaijuittuq Marine Protected Area (MPA), the Canadian northernmost protected area.

Zooplankton-mediated processes participate in the regulation of the carbon and nitrogen pathways within aquatic ecosystems, and in the functioning of the ocean biological carbon pump that sequesters carbon out of the atmosphere (Ducklow et al., 2001). Combined with information on migration patterns and diet, our data on community structure, composition, size classes, and biomass distribution can help to formulate a preliminary view of the geographic variability of the role that zooplankton play in carbon flux in the North American Arctic waters. The large *Calanus* species, *Metridia longa*, and euphausiids are known to perform extensive diel and/or seasonal vertical migrations through which they actively transport carbon consumed in the surface layer to the deep ocean where it can be sequestered for a long time (Jónasdóttir et al., 2015; Darnis et al., 2017). *C. hyperboreus* alone transports during its seasonal vertical migrations a quantity of carbon comparable to the gravitational export of POC measured with sediment traps in the Amundsen Gulf (Darnis and Fortier, 2012), one of our zooplankton biomass hotspots. A similarly important contribution of the seasonal vertical migrations of *C. hyperboreus* to the biological carbon pump was found in the deep Fram Strait, Greenland, and in Iceland seas (Hirche, 1997; Visser et al., 2017). Therefore, we hypothesize that the other biomass hotspots described in this study, namely Lancaster Sound, the North Water Polynya and Baffin Bay, are also potentially important carbon sinks, due to deep waters, relatively high pelagic primary production, and the high share of long-range zooplankton vertical migrants operating an active flux of carbon. Following these conditions, the subarctic northern Labrador Sea should be an area where the oceanic boreal *C. finmarchicus* and arctic *C. hyperboreus* play a significant role in carbon export through their vertical migrations.

On the other hand, the carbon pump in shallow areas like the inner Mackenzie Shelf, the south Kitikmeot, Foxe Basin, and Hudson Bay would most likely be driven essentially by the gravitational (passive) POC export, due to low biomass and representation of large size vertical migrants. The less mobile but numerically dominant small omnivorous and detritivorous copepods mainly reduce the POC export by recycling organic carbon in the epipelagic layer

(Sampei et al., 2008). Moreover, zooplankton activity is expected to affect the level of pelagic-benthic coupling (Darnis et al., 2012). However, poor knowledge of the biogeography of North American Arctic benthos, particularly biomass distribution, makes verifying the relationship between zooplankton and benthos spatial patterns difficult. A proper assessment of the influence of zooplankton processes on the biogeochemical cycling of carbon in this vast and complex marine ecosystem requires a significant increase in our understanding of Arctic zooplankton biology, particularly diet diversity, phenology, seasonal variability of metabolism and carbon demand, migration patterns, overwintering depth, and mortality.

Conclusion

Recent scientific evidence indicates that marine species are expanding their distributional range northward into the Arctic, under the effects of climate change. This expansion has been well documented for zooplankton assemblages in the two main Arctic-Subarctic transition zones of the Bering-Chukchi and the Barents-Fram Strait systems (Basedow et al., 2018; Kim et al., 2020), and also along eastern Baffin Bay where boreal zooplankton are transported northward by the Atlantic-influenced West Greenland Current (Møller and Nielsen, 2020). There, the North Atlantic *Calanus finmarchicus* is replacing its larger arctic congeners *C. glacialis* and *C. hyperboreus*, with consequences higher up the food web. In contrast, we did not find any significant effect of Atlantic and Pacific taxa on zooplankton composition in the sector of the North American Arctic under study, the subarctic Hudson Complex, and the Labrador fjords, all areas through which cold arctic waters flow. Thus, except for the sub arctic Labrador Sea assemblage that had a strong Atlantic signature, the assemblages identified by this study can be considered as true arctic zooplankton communities, similar to the ones described by earlier arctic studies (Dunbar, 1953; Grainger, 1965).

This work provides a strong baseline against which we will be able to gauge changes in the zooplankton community structure over a vast region of the Arctic subject to intensified oceanographic Atlantification and Pacification at its eastern and western boundaries (Polyakov et al., 2020). Based on an unprecedented sampling resolution and geographic scale, our data reveal the complexities of the mechanisms maintaining connectivity within this large pelagic ecosystem and pinpoint the factors of geographic discontinuities in the zooplankton community distribution. We surmise that an interplay between zooplankton habitat preference and vertical distribution, and the presence of sills and shallow areas constraining the transport of mesopelagic species by underlying currents such as the Atlantic Water layer below a depth of 200 m, is responsible for the discrimination of the main zooplankton assemblages in the North American Arctic. The data underline the status of the central Amundsen Gulf, Lancaster Sound, the North Water, and western Baffin Bay as mesozooplankton biomass hotspots in deep (>300 m) habitats often near or in known polynyas. These areas have already been, or are still in the process of being, designated as Marine Protected Areas for the richness of their fauna. In these oceanic parts of the North American Arctic, the large herbivorous and arctic-endemic copepod *Calanus hyperboreus* represents >60% of the copepod biomass, highlighting its rank as a keystone species in the Arctic marine ecosystem. Thus, environmental disruptions affecting *C. hyperboreus* populations in this part of the Arctic should be monitored (Darnis et al., 2019).

We can only emphasize the need to increase sampling resolution in coastal areas that likely provide habitats for more zooplankton assemblages, some sustaining Arctic char stocks and dependent northern fisheries. Furthermore, plankton communities need to be better documented along the most heavily ice-covered sectors of the Northwest Passage, including M'Clure Strait, Viscount Melville Sound, The Queen Elizabeth Islands in the north of the CAA, and finally in the Gulf of Boothia, considered as an important feeding area for planktivorous bowhead whales.

Data accessibility statement

Mesozooplankton data in northern Baffin Bay: Polar Data Catalogue CCIN 10508. Mesozooplankton data in the Canadian Arctic Archipelago: Polar Data Catalogue CCIN 10510. Mesozooplankton data in the Labrador Sea and Canadian Arctic: Polar Data Catalogue CCIN 13168.

Supplemental files

The supplemental files for this article can be found as follows:

Figure S1. Annual time series of sea ice concentration at several sampling sites from 2005 to 2018.

Figure S2. Zooplankton sampling sites along the annual west-east tracks of the ship from 2005 to 2018.

Figure S3. Copepod biomass and areas of high density of vertebrate planktivores in the North American Arctic.

Figure S4. Copepod biomass and actual and proposed marine protected areas (MPA) in the North American Arctic.

Table S1. Depth, geographic coordinates, and sampling dates of the 409 stations sampled in the North American Arctic and eastern Subarctic.

Table S2. Abundance of the 201 taxa identified and copepod biomass averaged over the North American Arctic and eastern Subarctic.

Table S3. Spearman's rank correlations between pairs of environmental variables.

Table S4. Estimates of integrated abundance of zooplankton and biomass of copepods in various arctic and subarctic regions.

Acknowledgments

We thank officers, crew members, scientists, and chief scientists for their assistance in the collection of samples on board the Canadian research icebreaker CCGS *Amundsen*. Some of the data presented herein were made available by the Amundsen Science program, which was supported by the Canada Foundation for Innovation and Natural Sciences and Engineering Research Council of Canada. The views expressed in this publication do not

necessarily represent the views of Amundsen Science or that of its partners. Zooplankton samples were collected under various projects (CFL, Green Edge, Kitikmeot Marine Ecosystem Study, Malina, ISECOLD) funded notably by ArcticNet, the W. Garfield Weston Foundation, the Natural Sciences and Engineering Research Council of Canada (NSERC), the Canada Foundation for Innovation (CFI), Fisheries and Oceans Canada, and the International Polar Year (IPY). This work was supported by the Crown-Indigenous Relations and Northern Affairs Canada. This is a contribution to Québec-Océan, the Canada Research Chair on the response of arctic marine ecosystems to climate warming, and to the Ocean Frontier Institute through the Canada First Research Excellence Fund. The expedition reports since 2005 and research licences obtained for ArcticNet expeditions since 2018 onboard the CCGS Amundsen are available at https://amundsenscience.com/expeditions/past-expeditions/.

Competing interests

The authors have no competing interests to declare.

Author contributions

Contributed to conception and design: GD, LF, MG, TB, MB, DC.

Contributed to acquisition of data: GD, MG, LF, TD, CA, PM, TB, MB, DC.

Contributed to analysis and interpretation of data: GD, MG, LF, PM, TB, MB, DC.

Drafted and/or revised the article: GD, MG, LF, TD, CA, PM, TB, MB, DC.

Approved the submitted version for publication: GD, MG, TD, CA, PM, TB, MB, DC.

References

Ardyna, M, **Arrigo, KR.** 2020. Phytoplankton dynamics in a changing Arctic Ocean. *Nature Climate Change* **10**(10): 892–903.

Ardyna, M, **Gosselin, M**, **Michel, C**, **Poulin, M**, **Tremblay, J.** 2011. Environmental forcing of phytoplankton community structure and function in the Canadian high Arctic: Contrasting oligotrophic and eutrophic regions. *Marine Ecology Progress Series* **442**: 37–57.

Armitage, TWK, **Manucharyan, GE**, **Petty, AA**, **Kwok, R**, **Thompson, AF.** 2020. Enhanced eddy activity in the Beaufort Gyre in response to sea ice loss. *Nature Communications* **11**(1): 761. DOI: http://dx.doi.org/10.1038/s41467-020-14449-z.

Ashjian, CJ, **Campbell, RG**, **Welch, HE**, **Butler, M**, **Van Keuren, D.** 2003. Annual cycle in abundance, distribution, and size in relation to hydrography of important copepod species in the Western Arctic Ocean. *Deep Sea Research Part I: Oceanographic Research* **50**: 1235–1261.

Auel, H, **Hagen, W.** 2002. Mesozooplankton community structure, abundance and biomass in the central Arctic Ocean. *Marine Biology* **140**(5): 1013–1021.

Babin, M, **Bélanger, S**, **Ellingsen, I**, **Forest, A**, **Le Fouest, V**, **Lacour, T**, **Ardyna, M**, **Slagstad, D.** 2015. Estimation of primary production in the Arctic Ocean using ocean colour remote sensing and coupled physical–biological models: Strengths, limitations and how they compare. *Progress in Oceanography* **139**: 197–220.

Back, D-Y, **Ha, S-Y**, **Else, B**, **Hanson, M**, **Jones, SF**, **Shin, K-H**, **Tatarek, A**, **Wiktor, JM**, **Cicek, N**, **Alam, S**, **Mundy, CJ.** 2021. On the impact of wastewater effluent on phytoplankton in the Arctic coastal zone: A case study in the Kitikmeot sea of the Canadian Arctic. *Science of the Total Environment* **764**: 143861. DOI: http://dx.doi.org/10.1016/j.scitotenv.2020.143861.

Baird, A, **Bickham, JW**. 2021. The stocks of bowheads, in George, JC, Thewissen, JGM eds., *The Bowhead Whale Balaena mysticetus: Biology and human interactions*. Amsterdam, The Netherlands: Elsevier.

Basedow, SL, **Sundfjord, A**, **von Appen, W-J**, **Halvorsen, E**, **Kwasniewski, S**, **Reigstad, M.** 2018. Seasonal variation in transport of zooplankton into the Arctic Basin through the Atlantic gateway, Fram Strait. *Frontiers in Marine Science* **5**: 194. DOI: http://dx.doi.org/10.3389/fmars.2018.00194.

Beaupré-Laperrière, A, **Mucci, A**, **Thomas, H.** 2020. The recent state and variability of the carbonate system of the Canadian Arctic Archipelago and adjacent basins in the context of ocean acidification. *Biogeosciences* **17**(14): 3923–3942.

Bluhm, BA, **Janout, MA**, **Danielson, SL**, **Ellingsen, I**, **Gavrilo, M**, **Grebmeier, JM**, **Hopcroft, RR**, **Iken, KB**, **Ingvaldsen, RB**, **Jørgensen, LL**, **Kosobokova, KN**, **Kwok, R**, **Polyakov, IV**, **Renaud, PE**, **Carmack, IC.** 2020. The Pan-Arctic continental slope: Sharp gradients of physical processes affect pelagic and benthic ecosystems. *Frontiers in Marine Science* **7**: 544386. DOI: http://dx.doi.org/10.3389/fmars.2020.544386.

Botterell, ZLR, **Bergmann, M**, **Hildebrandt, N**, **Krumpen, T**, **Steinke, M**, **Thompson, RC**, **Lindeque, PK.** 2022. Microplastic ingestion in zooplankton from the Fram Strait in the Arctic. *Science of the Total Environment* **831**: 154886. DOI: http://dx.doi.org/10.1016/j.scitotenv.2022.154886.

Bouchard, C, **Fortier, L.** 2020. The importance of *Calanus glacialis* for the feeding success of young Polar cod: A circumpolar synthesis. *Polar Biology* **43**(8): 1095–1107.

Bouchard, C, **Geoffroy, M**, **LeBlanc, M**, **Fortier, L.** 2018. Larval and adult fish assemblages along the Northwest Passage: The shallow Kitikmeot and the ice-covered Parry Channel as potential barriers to dispersal. *Arctic Science* **4**(4): 781–793.

Bray, JR, **Curtis, JT.** 1957. An ordination of the upland forest communities of Southern Wisconsin. *Ecological Monographs* **27**(4): 325–349.

Brown, T, **Reimer, K**, **Sheldon, T**, **Bell, T**, **Bentley, S**, **Pienitz, R**, **Gosselin, M**, **Blais, M**, **Carpenter, M**, **Estrada, E**, **Richerol, T**, **Kahlmeyer, E**, **Luque, S**, **Sjare, B**, **Fisk, A**, **Iverson, S.** 2012. A first look at Nunatsiavut Kangidualuk ('fjord') ecosystems, in

Allard, M, Lemay, M eds., *Nunavik and Nunatsiavut: From science to policy. An Integrated Regional Impact Study (IRIS) of climate change and modernization*. Quebec City, Canada: ArcticNet Inc.

Carmack, E, **Chapman, DC.** 2003. Wind-driven shelf/basin exchange on an Arctic shelf: The joint roles of ice cover extent and shelf-break bathymetry. *Geophysical Research Letters* **30**(14): 1778. DOI: http://dx.doi.org/10.1029/2003GL017526.

Carmack, EC, **Macdonald, RW.** 2002. Oceanography of the Canadian Shelf of the Beaufort Sea: A setting for marine life. *Arctic* **55**: 29–45.

Carroll, GM, **George, JC**, **Lowry, LF**, **Coyle, KO.** 1987. Bowhead whale (*Balaena mysticetus*) feeding near Point Barrow, Alaska, during the 1985 spring migration. *Arctic* **40**(2): 105–110.

Chambers, C, **MacDonell, D**. 2012. *Ecological overview and assessment report for the Anuniaqvia Niqiqyuam area of interest*. Winnipeg, Canada: North/South Consultants Inc.

Clarke, K, **Warwick, R**. 2001. *Change in marine communities: An approach to statistical analysis and interpretation*. Plymouth, UK: Primer-E Ltd.

Clay, S, **Peña, A**, **DeTracey, B**, **Devred, E.** 2019. Evaluation of satellite-based algorithms to retrieve chlorophyll-a concentration in the Canadian Atlantic and Pacific Oceans. *Remote Sensing* **11**(22): 2609. DOI: http://dx.doi.org/10.3390/rs11222609.

Cuny, J, **Rhines, P**, **Niiler, P**, **Bacon, S.** 2002. Labrador Sea boundary currents and the fate of the Irminger Sea water. *Journal of Physical Oceanography* **32**: 627–647.

Darnis, G, **Barber, DG**, **Fortier, L.** 2008. Sea ice and the onshore–offshore gradient in pre-winter zooplankton assemblages in Southeastern Beaufort Sea. *Journal of Marine Systems* **74**(3): 994–1011.

Darnis, G, **Fortier, L.** 2012. Zooplankton respiration and the export of carbon at depth in the Amundsen Gulf (Arctic Ocean). *Journal of Geophysical Research: Oceans* **117**: C04013. DOI: http://dx.doi.org/10.1029/2011JC007374.

Darnis, G, **Fortier, L.** 2014. Temperature, food and the seasonal vertical migration of key arctic copepods in the thermally stratified Amundsen Gulf (Beaufort Sea, Arctic Ocean). *Journal of Plankton Research* **36**(4): 1092–1108.

Darnis, G, **Hobbs, L**, **Geoffroy, M**, **Grenvald, JC**, **Renaud, PE**, **Berge, J**, **Cottier, F**, **Kristiansen, S**, **Daase, M**, **Søreide, JE**, **Wold, A**, **Morata, N**, **Gabrielsen, T.** 2017. From polar night to midnight sun: Diel vertical migration, metabolism and biogeochemical role of zooplankton in a high arctic fjord (Kongsfjorden, Svalbard). *Limnology and Oceanography* **62**(4): 1586–1605.

Darnis, G, **Robert, D**, **Pomerleau, C**, **Link, H**, **Archambault, P**, **Nelson, RJ**, **Geoffroy, M**, **Tremblay, J-É**, **Lovejoy, C**, **Ferguson, SH**, **Hunt, BPV**, **Fortier, L.** 2012. Current state and trends in Canadian Arctic marine ecosystems: II. Heterotrophic food web, pelagic-benthic coupling, and biodiversity. *Climatic Change* **115**(1): 179–205.

Darnis, G, **Wold, A**, **Falk-Petersen, S**, **Graeve, M**, **Fortier, L.** 2019. Could offspring predation offset the successful reproduction of the Arctic copepod *Calanus hyperboreus* under reduced sea-ice cover conditions? *Progress in Oceanography* **170**: 107–118.

Dezutter, T, **Lalande, C**, **Darnis, G**, **Fortier, L.** 2021. Seasonal and interannual variability of the Queen Maud Gulf ecosystem derived from sediment trap measurements. *Limnology and Oceanography* **66**(S1): S411–S426.

Druon, J-N, **Hélaouët, P**, **Beaugrand, G**, **Fromentin, J-M**, **Palialexis, A**, **Hoepffner, N.** 2019. Satellite-based indicator of zooplankton distribution for global monitoring. *Scientific Reports* **9**(1): 4732. DOI: http://dx.doi.org/10.1038/s41598-019-41212-2.

Ducklow, HW, **Steinberg, DK**, **Buesseler, KO.** 2001. Upper ocean carbon export and the biological pump. *Oceanography* **14**(4): 50–58.

Dunbar, MJ. 1953. Arctic and subarctic marine ecology: Immediate problems. *Arctic* **6**(2): 75–90.

Environment and Climate Change in Canada. 2021. Canadian environmental sustainability indicators: Sea ice in Canada. Available at https://www.canada.ca/en/environment-climate-change/services/environmental-indicators/sea-ice.html. Accessed 08 April 2022.

Ershova, EA, **Hopcroft, RR**, **Kosobokova, KN.** 2015. Inter-annual variability of summer mesozooplankton communities of the Western Chukchi Sea: 2004–2012. *Polar Biology* **38**(9): 1461–1481.

Falardeau, M, **Bouchard, C**, **Robert, D**, **Fortier, L.** 2017. First records of Pacific sand lance (*Ammodytes hexapterus*) in the Canadian Arctic Archipelago. *Polar Biology* **40**(11): 2291–2296.

Falk-Petersen, S, **Mayzaud, P**, **Kattner, G**, **Sargent, JR.** 2009. Lipids and life strategy of Arctic *Calanus*. *Marine Biology Research* **5**(1): 18–39.

Forest, A, **Galindo, V**, **Darnis, G**, **Pineault, S**, **Lalande, C**, **Tremblay, J-É**, **Fortier, L.** 2010. Carbon biomass, elemental ratios (C: N) and stable isotopic composition (δ13C, δ15 N) of dominant calanoid copepods during the winter-to-summer transition in the Amundsen Gulf (Arctic Ocean). *Journal of Plankton Research* **33**(1): 161–178.

Forest, A, **Tremblay, J-É**, **Gratton, Y**, **Martin, J**, **Gagnon, J**, **Darnis, G**, **Sampei, M**, **Fortier, L**, **Ardyna, M**, **Gosselin, M**, **Hattori, H**, **Nguyen, D**, **Maranger, R**, **Vaqué, D**, **Marrasé, C**, **Pedrós-Alió, C**, **Sallon, A**, **Michel, C**, **Kellogg, C**, **Deming, J**, **Shadwick, E**, **Thomas, H**, **Link, H**, **Archambault, P**, **Piepenburg, D.** 2011. Biogenic carbon flows through the planktonic food web of the Amundsen Gulf (Arctic Ocean): A synthesis of field measurements and inverse modeling analyses. *Progress in Oceanography* **91**(4): 410–436.

Fortier, M, **Fortier, L**, **Michel, C**, **Legendre, L.** 2002. Climatic and biological forcing of vertical flux and

biogenic particles under seasonal Arctic sea ice. *Marine Ecology Progress Series* **225**: 1–16.

Fortune, SME, **Ferguson, SH**, **Trites, AW**, **Hudson, JM**, **Baumgartner, MF.** 2020. Bowhead whales use two foraging strategies in response to fine-scale differences in zooplankton vertical distribution. *Scientific Reports* **10**(1): 20249. DOI: http://dx.doi.org/10.1038/s41598-020-76071-9.

Grainger, E. 1965. Zooplankton from the Arctic Ocean and adjacent Canadian waters. *Journal of the Fisheries Research Board of Canada* **22**: 543–564.

Greer, AT, **Lehrter, JC**, **Binder, BM**, **Nayak, AR**, **Barua, R**, **Rice, AE**, **Cohen, JH**, **McFarland, MN**, **Hagemeyer, A**, **Stockley, ND**, **Boswell, KM**, **Shulman, I**, **deRada, S**, **Penta, B.** 2020. High-resolution sampling of a broad marine life size spectrum reveals differing size- and composition-based associations with physical oceanographic structure. *Frontiers in Marine Science* **7**: 542701. DOI: http://dx.doi.org/10.3389/fmars.2020.542701.

Halfter, S, **Cavan, EL**, **Swadling, KM**, **Eriksen, RS**, **Boyd, PW.** 2020. The role of zooplankton in establishing carbon export regimes in the southern ocean—A comparison of two representative case studies in the subantarctic region. *Frontiers in Marine Science* **7**: 567917. DOI: http://dx.doi.org/10.3389/fmars.2020.567917.

Halsband, C, **Dix, MF**, **Sperre, KH**, **Reinardy, HC.** 2021. Reduced pH increases mortality and genotoxicity in an Arctic coastal copepod, *Acartia longiremis*. *Aquatic Toxicology* **239**: 105961. DOI: http://dx.doi.org/10.1016/j.aquatox.2021.105961.

Hamilton, CD, **Lydersen, C**, **Aars, J**, **Acquarone, M**, **Atwood, T**, **Baylis, A**, **Biuw, M**, **Boltunov, AN**, **Born, EW**, **Boveng, P**, **Brown, TM**, **Cameron, M**, **Citta, J**, **Crawford, J**, **Dietz, R**, **Elias, J**, **Ferguson, SH**, **Fisk, A**, **Folkow, LP**, **Frost, KJ**, **Glazov, DM**, **Granquist, SM**, **Gryba, R**, **Harwood, L**, **Haug, T**, **Heide-Jørgensen, MP**, **Hussey, NE**, **Kalinek, J**, **Laidre, KL**, **Litovka, DI**, **London, JM**, **Loseto, LL**, **MacPhee, S**, **Marcoux, M**, **Matthews, CJD**, **Nilssen, K**, **Nordøy, ES**, **O'Corry-Crowe, G**, **Øien, N**, **Olsen, MT**, **Quakenbush, L**, **Rosing-Asvid, A**, **Semenova, V**, **Shelden, KEW**, **Shpak, OV**, **Stenson, G**, **Storrie, L**, **Sveegaard, S**, **Teilmann, J**, **Ugarte, F**, **Von Duyke, AL**, **Watt, C**, **Wiig, Ø**, **Wilson, RR**, **Yurkowski, DJ**, **Kovacs, KM.** 2022. Marine mammal hotspots across the circumpolar Arctic. *Diversity and Distributions*. DOI: http://dx.doi.org/10.1111/ddi.13543.

Harrison, WG, **Børsheim, KY**, **Li, WKW**, **Maillet, GL**, **Pepin, P**, **Sakshaug, E**, **Skogen, MD**, **Yeats, PA.** 2013. Phytoplankton production and growth regulation in the Subarctic North Atlantic: A comparative study of the Labrador Sea-Labrador/Newfoundland shelves and Barents/Norwegian/Greenland seas and shelves. *Progress in Oceanography* **114**: 26–45.

Hillman, JR, **Lundquist, CJ**, **Thrush, SF.** 2018. The challenges associated with connectivity in ecosystem processes. *Frontiers in Marine Science* **5**: 364. DOI: http://dx.doi.org/10.3389/fmars.2018.00364.

Hirche, HJ. 1997. Life cycle of the copepod *Calanus hyperboreus* in the Greenland Sea. *Marine Biology* **128**(4): 607–618.

Hop, H, **Assmy, P**, **Wold, A**, **Sundfjord, A**, **Daase, M**, **Duarte, P**, **Kwasniewski, S**, **Gluchowska, M**, **Wiktor, JM**, **Tatarek, A**, **Wiktor, J**, **Kristiansen, S**, **Fransson, A**, **Chierici, M**, **Vihtakari, M.** 2019. Pelagic ecosystem characteristics across the Atlantic water boundary current from Rijpfjorden, Svalbard, to the Arctic Ocean during summer (2010–2014). *Frontiers in Marine Science* **6**: 181. DOI: http://dx.doi.org/10.3389/fmars.2019.00181.

Hopcroft, RR, **Clarke, C**, **Nelson, RJ**, **Raskoff, KA.** 2005. Zooplankton communities of the Arctic's Canada Basin: The contribution by smaller taxa. *Polar Biology* **28**(3): 198–206.

Howell, SEL, **Wohlleben, T**, **Dabboor, M**, **Derksen, C**, **Komarov, A**, **Pizzolato, L.** 2013. Recent changes in the exchange of sea ice between the Arctic Ocean and the Canadian Arctic Archipelago. *Journal of Geophysical Research: Oceans* **118**(7): 3595–3607.

Jónasdóttir, SH, **Visser, AW**, **Richardson, K**, **Heath, MR.** 2015. Seasonal copepod lipid pump promotes carbon sequestration in the deep North Atlantic. *Proceedings of the National Academy of Sciences* **112**(39): 12122–12126.

Karnovsky, N, **Brown, Z**, **Welcker, J**, **Harding, A**, **Walkusz, W**, **Cavalcanti, A**, **Hardin, J**, **Kitaysky, A**, **Gabrielsen, G**, **Grémillet, D.** 2011. Inter-colony comparison of diving behavior of an Arctic top predator: Implications for warming in the Greenland Sea. *Marine Ecology Progress Series* **440**: 229–240.

Kim, J-H, **Cho, K-H**, **La, HS**, **Choy, EJ**, **Matsuno, K**, **Kang, S-H**, **Kim, W**, **Yang, EJ.** 2020. Mass occurrence of Pacific copepods in the Southern Chukchi Sea during summer: Implications of the high-temperature Bering summer water. *Frontiers in Marine Science* **7**: 612. DOI: http://dx.doi.org/10.3389/fmars.2020.00612.

Kimmerer, WJ, **Gross, ES**, **MacWilliams, ML.** 2014. Tidal migration and retention of estuarine zooplankton investigated using a particle-tracking model. *Limnology and Oceanography* **59**(3): 901–916.

Kosobokova, KN, **Hanssen, H**, **Hirche, HJ**, **Knickmeier, K.** 1997. Composition and distribution of zooplankton in the Laptev Sea and adjacent Nansen Basin during summer, 1993. *Polar Biology* **19**(1): 63–76.

Kruskal, JB, **Wish, M.** 1978. *Multidimensional scaling*. Thousand Oaks, CA: Sage Publications. (Series on quantitative applications in the social sciences).

Lancaster Sound National Marine Conservation Area Feasibility Assessment Steering Committee. 2017. A national marine conservation area proposal for Lancaster Sound. Feasibility assessment report. Available at https://www.qia.ca/wp-content/uploads/2017/08/NMCA-Propossal-for-Lancaster-Sound-ENG-April-4.pdf. Accessed 08 April 2022.

Lee, SH, **Whitledge, TE.** 2005. Primary and new production in the deep Canada Basin during summer 2002. *Polar Biology* **28**(3): 190–197.

Loewen, T, **Hornby, C**, **Johnson, M**, **Chambers, C**, **Dawson, K**, **Macdonell, D**, **Bernhardt, W**, **Gnanapragasam, R**, **Pierrejean, M**, **Choy, E**. 2020. Ecological and biophysical overview of the Southampton Island ecologically and biologically significant area in support of the identification of an area of interest. Ottawa, Canada: Fisheries and Oceans Canada. DFO Canadian Scientific Advisory Secretariat 2020/032. Available at https://publications.gc.ca/site/eng/9.890957/publication.html. Accessed 08 April 2022.

Martin, J, **Tremblay, J**, **Gagnon, J**, **Tremblay, G**, **Lapoussière, A**, **Jose, C**, **Poulin, M**, **Gosselin, M**, **Gratton, Y**, **Michel, C.** 2010. Prevalence, structure and properties of subsurface chlorophyll maxima in Canadian Arctic waters. *Marine Ecology Progress Series* **412**: 69–84.

Matsuno, K, **Yamaguchi, A**, **Fujiwara, A**, **Onodera, J**, **Watanabe, E**, **Harada, N**, **Kikuchi, T.** 2015. Seasonal changes in the population structure of dominant planktonic copepods collected using a sediment trap moored in the Western Arctic Ocean. *Journal of Natural History* **49**(45–48): 2711–2726.

McLaughlin, FA, **Carmack, EC**, **Ingram, RG**, **Williams, WJ**, **Michel, C**. 2004. Oceanography of the Northwest Passage, in Robinson, AR, Brink, KH eds., *The sea* (vol. 14). Boston, MA: Harvard College.

Michel, C, **Hamilton, J**, **Hansen, E**, **Barber, D**, **Reigstad, M**, **Iacozza, J**, **Seuthe, L**, **Niemi, A.** 2015. Arctic Ocean outflow shelves in the changing Arctic: A review and perspectives. *Progress in Oceanography* **139**: 66–88.

Møller, E, **Johansen, K**, **Agersted, M**, **Rigét, F**, **Clausen, D**, **Larsen, J**, **Lyngs, P**, **Middelbo, A**, **Mosbech, A.** 2018. Zooplankton phenology may explain why the North Water Polynya region is such an important breeding area for little auks. *Marine Ecology Progress Series* **605**: 207–223.

Møller, EF, **Nielsen, TG.** 2020. Borealization of Arctic zooplankton—Smaller and less fat zooplankton species in Disko Bay, Western Greenland. *Limnology and Oceanography* **65**(6): 1175–1188.

Mudryk, LR, **Derksen, C**, **Howell, S**, **Laliberté, F**, **Thackeray, C**, **Sosspedra-Alfonso, R**, **Vionnet, V**, **Kushner, PJ**, **Brown, R.** 2018. Canadian snow and sea ice: Historical trends and projections. *The Cryosphere* **12**(4): 1157–1176.

Mumm, N. 1991. Zur sommerlichen verteilung des mesozooplanktons im Nansen-Becken, Nordpolarmeer (Berichte zur Polarforschung) = On the summerly distribution of mesozooplankton in the Nansen Basin, Arctic Ocean (Reports on Polar Research). Bremerhaven, Germany: Alfred Wegener Institute for Polar and Marine Research.

Münchow, A, **Falkner, KK**, **Melling, H.** 2015. Baffin island and West Greenland current systems in Northern Baffin Bay. *Progress in Oceanography* **132**: 305–317.

Nelson, RJ, **Carmack, EC**, **McLaughlin, FA**, **Cooper, GA.** 2009. Penetration of Pacific zooplankton into the Western Arctic Ocean tracked with molecular population genetics. *Marine Ecology Progress Series* **381**: 129–138.

Niemi, A, **Bednaršek, N**, **Michel, C**, **Feely, R**, **Williams, W**, **Azetsu-Scott, K**, **Walkusz, W**, **Reist, J.** 2021. Biological impact of ocean acidification in the Canadian Arctic: Widespread severe pteropod shell dissolution in Amundsen Gulf. *Frontiers in Marine Science* **8**: 600184. DOI: http://dx.doi.org/10.3389/fmars.2021.600184.

Niemi, A, **Ferguson, S**, **Hedges, K**, **Melling, H**, **Michel, C**, **Ayles, B**, **Azetsu-Scott, K**, **Coupel, P**, **Deslauriers, D**, **Devred, E**, **Doniol-Valcroze, T**, **Dunmall, K**, **Eert, J**, **Galbraith, P**, **Geoffroy, M**, **Gilchrist, G**, **Hennin, H**, **Howland, K**, **Kendall, M**, **Zimmerman, S.** 2019. State of Canada's Arctic seas. Winnipeg, Canada: Fisheries and Oceans Canada. Canadian Technical Report of Fisheries and Aquatic Sciences 3344.

Oziel, L, **Baudena, A**, **Ardyna, M**, **Massicotte, P**, **Randelhoff, A**, **Sallée, JB**, **Ingvaldsen, RB**, **Devred, E**, **Babin, M.** 2020. Faster Atlantic currents drive poleward expansion of temperate phytoplankton in the Arctic Ocean. *Nature Communications* **11**(1): 1705. DOI: http://dx.doi.org/10.1038/s41467-020-15485-5.

Pedersen, CE, **Falk, K.** 2001. Chick diet of dovekies *Alle alle* in Northwest Greenland. *Polar Biology* **24**(1): 53–58.

Pendleton, DE, **Holmes, EE**, **Redfern, J**, **Zhang, J.** 2020. Using modelled prey to predict the distribution of a highly mobile marine mammal. *Diversity and Distributions* **26**(11): 1612–1626.

Pikialasorsuaq Commission. 2017. *People of the Ice Bridge: The future of the Pikialasorsuaq*. Ottawa, Canada: Inuit Circumpolar Council Canada. Available at https://repository.oceanbestpractices.org/handle/11329/1826. Accessed 08 April 2022.

Polyakov, IV, **Alkire, MB**, **Bluhm, BA**, **Brown, KA**, **Carmack, EC**, **Chierici, M**, **Danielson, SL**, **Ellingsen, I**, **Ershova, EA**, **Gårdfeldt, K**, **Ingvaldsen, RB**, **Pnyushkov, AV**, **Slagstad, D**, **Wassmann, P.** 2020. Borealization of the Arctic Ocean in response to anomalous advection from sub-Arctic seas. *Frontiers in Marine Science* **7**: 491. DOI: http://dx.doi.org/10.3389/fmars.2020.00491.

Pomerleau, C, **Nelson, RJ**, **Hunt, BPV**, **Sastri, AR**, **Williams, WJ.** 2014. Spatial patterns in zooplankton communities and stable isotope ratios (δ13C and δ15 N) in relation to oceanographic conditions in the sub-Arctic Pacific and western Arctic regions during the summer of 2008. *Journal of Plankton Research* **36**(3): 757–775.

Pomerleau, C, **Winkler, G**, **Sastri, AR**, **Nelson, RJ**, **Vagle, S**, **Lesage, V**, **Ferguson, SH.** 2011. Spatial patterns in zooplankton communities across the eastern

Canadian sub-Arctic and Arctic waters: Insights from stable carbon (δ13C) and nitrogen (δ15 N) isotope ratios. *Journal of Plankton Research* **33**(12): 1779–1792.

Richter, DJ, **Watteaux, R**, **Vannier, T**, **Leconte, J**, **Frémont, P**, **Reygondeau, G**, **Maillet, N**, **Henry, N**, **Benoit, G**, **Silva, OD**, **Delmont, TO**, **Fernàndez-Guerra, A**, **Suweis, S**, **Narci, R**, **Berney, C**, **Eveillard, D**, **Gavory, F**, **Guidi, L**, **Labadie, K**, **Mahieu, E**, **Poulain, J**, **Romac, S**, **Roux, S**, **Dimier, C**, **Kandels, S**, **Picheral, M**, **Searson, S**, **Coordinators, TO**, **Pesant, S**, **Aury, J-M**, **Brum, JR**, **Lemaitre, C**, **Pelletier, E**, **Bork, P**, **Sunagawa, S**, **Lombard, F**, **Karp-Boss, L**, **Bowler, C**, **Sullivan, MB**, **Karsenti, E**, **Mariadassou, M**, **Probert, I**, **Peterlongo, P**, **Wincker, P**, **de Vargas, C**, **d'Alcalà, MR**, **Iudicone, D**, **Jaillon, O.** 2020. Genomic evidence for global ocean plankton biogeography shaped by large-scale current systems. *BioRxiv*. DOI: http://dx.doi.org/10.1101/867739.

Ridenour, NA, **Hu, X**, **Sydor, K**, **Myers, PG**, **Barber, DG.** 2019. Revisiting the circulation of Hudson Bay: Evidence for a seasonal pattern. *Geophysical Research Letters* **46**(7): 3891–3899.

Ringuette, M, **Fortier, L**, **Fortier, M**, **Runge, JA**, **Bélanger, S**, **Larouche, P**, **Weslawski, J-M**, **Kwasniewski, S.** 2002. Advanced recruitment and accelerated population development in Arctic calanoid copepods of the North Water. *Deep Sea Research Part II: Topical Studies in Oceanography* **49**(22): 5081–5099.

Rochet, M, **Grainger, EH.** 1988. Community structure of zooplankton in Eastern Hudson Bay. *Canadian Journal of Zoology* **66**(7): 1626–1630.

Rudels, B. 2015. Arctic Ocean circulation, processes and water masses: A description of observations and ideas with focus on the period prior to the International Polar Year 2007–2009. *Progress in Oceanography* **132**: 22–67.

Sampei, M, **Forest, A**, **Sasaki, H**, **Hattori, H**, **Makabe, R**, **Fukuchi, M**, **Fortier, L.** 2008. Attenuation of the vertical flux of copepod fecal pellets under Arctic sea ice: Evidence for an active detrital food web in winter. *Polar Biology* **32**: 225–232.

Schmid, MS, **Cowen, RK**, **Robinson, K**, **Luo, JY**, **Briseño-Avena, C**, **Sponaugle, S.** 2020. Prey and predator overlap at the edge of a mesoscale eddy: Fine-scale, in-situ distributions to inform our understanding of oceanographic processes. *Scientific Reports* **10**(1): 921. DOI: http://dx.doi.org/10.1038/s41598-020-57879-x.

Schulze, L, **Pickart, R.** 2012. Seasonal variation of upwelling in the Alaskan Beaufort Sea: Impact of sea ice cover. *Journal of Geophysical Research (Oceans)* **117**(C6): 6022. DOI: http://dx.doi.org/10.1029/2012JC007985.

Smoot, CA, **Hopcroft, RR.** 2016. Cross-shelf gradients of epipelagic zooplankton communities of the Beaufort Sea and the influence of localized hydrographic features. *Journal of Plankton Research* **39**(1): 65–78.

Søreide, J, **Leu, E**, **Berge, J**, **Graeve, M**, **Falk-Petersen, S.** 2010. Timing of blooms, algal food quality and *Calanus glacialis* reproduction and growth in a changing Arctic. *Global Change Biology* **16**: 3154–3163.

Thor, P, **Bailey, A**, **Dupont, S**, **Calosi, P**, **Søreide, JE**, **De Wit, P**, **Guscelli, E**, **Loubet-Sartrou, L**, **Deichmann, IM**, **Candee, MM**, **Svensen, C**, **King, AL**, **Bellerby, RGJ.** 2018. Contrasting physiological responses to future ocean acidification among Arctic copepod populations. *Global Change Biology* **24**(1): e365–e377.

Tremblay, J-É, **Hattori, H**, **Michel, C**, **Ringuette, M**, **Mei, Z-P**, **Lovejoy, C**, **Fortier, L**, **Hobson, KA**, **Amiel, D**, **Cochran, K.** 2006. Trophic structure and pathways of biogenic carbon flow in the eastern North Water Polynya. *Progress in Oceanography* **71**(2): 402–425.

Tremblay, J-É, **Lee, J**, **Gosselin, M**, **Bélanger, S.** 2019. Nutrient dynamics and marine biological productivity in the greater Hudson Bay marine region, in Kuzyk, ZZ, Candlish, L eds., *From science to policy in the Greater Hudson Bay Marine Region: An Integrated Regional Impact Study (IRIS) of climate change and modernization*. Quebec City, Canada: ArcticNet Inc.

Ulrich, KL, **Tallman, RF.** 2021. The capelin invasion: Evidence for a trophic shift in Arctic char populations from the Cumberland Sound region, Nunavut, Canada. *Arctic Science* **7**(2): 413–435.

Visser, AW, **Grønning, J**, **Jónasdóttir, SH.** 2017. *Calanus hyperboreus* and the lipid pump. *Limnology and Oceanography* **62**(3): 1155–1165.

Walkusz, W, **Paulic, J**, **Kwasniewski, S**, **Williams, W**, **Wong, S**, **Papst, M.** 2009. Distribution, diversity and biomass of summer zooplankton from the coastal Canadian Beaufort Sea. *Polar Biology* **33**: 321–335.

Wang, K, **Munson, KM**, **Beaupré-Laperrière, A**, **Mucci, A**, **Macdonald, RW**, **Wang, F.** 2018. Subsurface seawater methylmercury maximum explains biotic mercury concentrations in the Canadian Arctic. *Scientific Report* **8**(1): 14465. DOI: http://dx.doi.org/10.1038/s41598-018-32760-0.

Wang, Q, **Myers, PG**, **Hu, X**, **Bush, ABG.** 2012. Flow constraints on pathways through the Canadian Arctic Archipelago. *Atmosphere-Ocean* **50**(3): 373–385.

Wong, SNP, **Gjerdrum, C**, **Morgan, KH**, **Mallory, ML.** 2014. Hotspots in cold seas: The composition, distribution, and abundance of marine birds in the North American Arctic. *Journal of Geophysical Research: Oceans* **119**(3): 1691–1705.

Zhang, J, **Weijer, W**, **Steele, M**, **Cheng, W**, **Verma, T**, **Veneziani, M.** 2021. Labrador Sea freshening linked to Beaufort Gyre freshwater release. *Nature Communications* **12**(1): 1229. DOI: http://dx.doi.org/10.1038/s41467-021-21470-3.

How to cite this article: Darnis, G, Geoffroy, M, Dezutter, T, Aubry, C, Massicotte, P, Brown, T, Babin, M, Cote, D, Fortier, L. 2022. Zooplankton assemblages along the North American Arctic: Ecological connectivity shaped by ocean circulation and bathymetry from the Chukchi Sea to Labrador Sea. *Elementa: Science of the Anthropocene* 10(1). DOI: https://doi.org/10.1525/elementa.2022.00053

Domain Editor-in-Chief: Jody W. Deming, University of Washington, Seattle, WA, USA

Guest Editor: Caroline Bouchard, Greenland Institute of Natural Resources, Nuuk, Greenland

Knowledge Domain: Ocean Science

Part of an Elementa Special Feature: Four Decades of Arctic Climate Change: A Tribute to Louis Fortier

Published: November 09, 2022 **Accepted:** September 09, 2022 **Submitted:** April 10, 2022

ELEMENTA Science of the Anthropocene

Elem Sci Anth is a peer-reviewed open access journal published by University of California Press.

OPEN ACCESS